

No evidence that natural selection has been less effective at removing deleterious mutations in Europeans than in West Africans

Ron Do^{1,2}, Daniel Balick^{1,3}, Heng Li^{1,2}, Ivan Adzhubei³, Shamil Sunyaev^{1,3} and David Reich^{1,2,4}

¹Broad Institute of Harvard and MIT, Cambridge, MA, USA, 02142; ²Department of Genetics, Harvard Medical School, Boston, MA 02115; ³Division of Genetics, Brigham & Women's Hospital, Harvard Medical School, Boston, MA, USA 02115; ⁴Howard Hughes Medical Institute, Harvard Medical School, Boston, MA, USA 02115

To whom correspondence should be addressed:

ssunyaev@rics.bwh.harvard.edu or reich@genetics.med.harvard.edu

Non-African populations have experienced major bottlenecks in the time since their split from West Africans, which has led to the hypothesis that natural selection to remove weakly deleterious mutations may have been less effective in non-Africans. To directly test this hypothesis, we measure the per-genome accumulation of deleterious mutations across diverse humans. We fail to detect any significant differences, but find that archaic Denisovans accumulated non-synonymous mutations at a higher rate than modern humans, consistent with the longer separation time of modern and archaic humans. We also revisit the empirical patterns that have been interpreted as evidence for less effective removal of deleterious mutations in non-Africans than in West Africans, and show they are not driven by differences in selection after population separation, but by neutral evolution.

The effectiveness with which natural selection removes deleterious mutations from a population depends not only on the selection coefficient (s) of a mutation, but on the product of this and the population size (N) (Ns , reviewed in 1). Thus, the rate at which deleterious alleles are removed from a population depends on demographic history. Profound demographic differences across humans are well documented. Founder events in the last hundred thousand years have reduced the nucleotide diversity (the number of differences per base pair between an individual's two chromosomes) in non-Africans by at least 20% relative to West Africans²⁻⁴, reflecting times

when the ancestors of non-Africans had relatively smaller population sizes. Similarly, the advent of agriculture in the last ten thousand years has led to rapid population expansions.

To investigate the empirical evidence for natural selection having differed in its effectiveness across human populations, past studies have contrasted mutation classes thought to be subject to little selection (synonymous mutations in genes) to those potentially subject to purifying selection (non-synonymous mutations)⁵⁻⁷. The most important study on this topic measured the proportion of polymorphic positions in genes that are non-synonymous in 20 European and 15 African American samples, and showed that while all such segregating sites have a reduced rate in non-Africans, the reduction is proportionally less for non-synonymous sites.⁵ Based on simulations, this observation was interpreted as being consistent with reduced effectiveness of selection against weakly deleterious alleles in European than in West African populations due to their smaller size since separation⁵. Subsequent studies have confirmed the empirical observation and favored a similar interpretation^{6,8,9}. These studies have clearly documented that there has been an interaction between the forces of natural selection and demographic history with regard to their effects on densities of non-synonymous sites^{5,6,8,9}. However, such observations do not necessarily imply that there have been differences in the effectiveness of selection between the two populations after the split. An alternative explanation is that in the common ancestral population of Europeans and West Africans, the average derived frequency for non-synonymous alleles was lower than for synonymous alleles, as negative selection places downward pressure on the frequency of derived alleles⁵. The different initial distributions for the two classes of alleles would have responded differently to the bottleneck that then occurred in European populations, simply because they started out with different shapes, an effect that would be expected to occur even in the absence of any differences in the effectiveness of selection between the two populations since they split.

The most direct way to contrast the effectiveness of selection between two populations is to sample a single haploid genome from each population, count all the differences, and measure which of the two lineages carries an excess. Any two lineages that are compared in this manner must, by definition, be separated by the same amount of time since their common ancestor, and are thus expected to harbor the same number of lineage-specific mutations in the absence of

selection or differences in mutation rate. In the presence of selection, however, mutations are removed from each lineage at a rate that depends on the product Ns , such that differences in the effectiveness of selection can be inferred from a detected asymmetry in the number of mutations in the two lineages. Here, we test for differences in the accumulation of mutations between two lineages by sampling one allele from population X and one from Y , determining the ancestral state based on the chimpanzee genome (*PanTro2*), and recording all the differences. We count the number of derived mutations in population X but not Y ($L_{X \text{ not } Y}$) and in Y but not X ($L_{Y \text{ not } X}$), and define a statistic $R_{X/Y} = L_{X \text{ not } Y} / L_{Y \text{ not } X}$. We average over all possible pairs of samples, and compute a standard error using a Weighted Block Jackknife to correct for correlation among neighboring sites (Methods)¹⁰. If selection has been equally effective since the split and mutation rates have been the same on the two lineages, $R_{X/Y}$ should be within a few standard errors from 1.

We measured $R_{\text{WestAfrica/Europe}}$ in four sequencing datasets: (1) coding regions of genes (exomes) from 15 African Americans and 20 European Americans⁵; (2) exomes from 1,089 individuals in the 1000 Genomes Project (1KG)¹¹; (3) exomes from 1,088 African Americans and 1,351 European Americans⁶, and (4) 24 whole genomes sequenced to high coverage^{12,13} (Table S1). As expected for sites unaffected by selection and for mutation rates being indistinguishable on the two lineages, $R_{\text{WestAfrica/Europe}}(\text{synonymous})$ is always within 2 standard errors of 1 (Table 1 and Table S1). However, $R_{\text{WestAfrica/Europe}}(\text{non-synonymous})$ is also indistinguishable from 1 (Table 1, Table 2, and Table S2). Thus, our empirical data provide no evidence that purging of weakly deleterious mutations has been less effective in Europeans than in West-Africans. This null result is consistent with the recently reported finding of ref.¹⁴ for similar population comparisons, which used a somewhat different approach. To generalize these results, we extended the analysis to a diverse set of human populations by computing $R_{X/Y}$ between all possible pairs of 5 diverse sub-Saharan African and 6 non-African populations¹³, and fourteen 1000 Genomes Project populations. We observe no significant differences for any pair despite profound differences in demographic history (Table 2 and Table S3).

To interpret these null findings, we carried out simulations using fitted models of the demographic histories of West African and European populations^{5,6,15}. (For most of our simulations, we assumed that mutations act additively although in Figure S1 we show that

qualitatively different patterns are expected for mutations that act recessively, a phenomenon that we explore in a separate study¹⁶.) The simulations predict that $R_{WestAfrica/Europe}$ will be below 0.95 when s is between -0.004 and -0.0004 (Figure 1). However, if many mutations have selection coefficients outside this range, the signal could be diluted to the point of not being detectable. Indeed, when we compute the expected value of $R_{WestAfrica/Europe}$ integrating over a previously fitted distribution of selection coefficients¹⁷, we find that $R_{WestAfrica/Europe}(non-synonymous)$ is expected to be 0.987, too close to 1 to be easily detectable given the standard errors of our empirical measurements (Table 1)¹⁸. We next attempted to boost our power by stratifying non-synonymous sites based on their predicted functional effects. The PolyPhen-2¹⁹ and SIFT²⁰ algorithms both predict function in a way that is dependent on the ancestral/derived status of allelic variants compared with the human reference genome, which has a particular ancestry at every segment that can bias measurements. We thus implemented a version of PolyPhen-2 that is independent of the allelic status of the human reference (Methods). We continue to observe no significant differences¹⁸ (Table 1, Table 2, Table S2, Table S3), although this null result may also reflect low power as when we infer the distribution of newly arising mutations for different PolyPhen-2 classes (Note S1), $R_{WestAfrica/Europe}$ is predicted to be 0.984-0.993 (Table S4).

To increase statistical power to detect any real differences in the net effectiveness of selection, we leveraged the fact that the population split between African and non-African populations occurred only in the last roughly one hundred thousand years. Mutations that arose prior to the population divergence are expected to dilute any true signal. We therefore computed a time-stratified $R_{African/non-African}$ -statistic, taking advantage of data from 4 experimentally phased African and 6 experimentally phased non-African genomes, all processed similarly¹³. We created pseudo-diploid genomes by merging 1 African and 1 non-African phased genome, for a total of $96 = (4 \times 2) \times (6 \times 2)$ comparisons, and then used the Pairwise Sequential Markovian Coalescent method (PSMC) to infer the local time since the most recent common ancestor (TMRCA) at each location, masking out the exome to avoid circularly using the same sites for inferring TMRCA and computing $R_{African/non-African}$. Table S5 shows that when we restrict to the subset of the genome with the lowest inferred TMRCA in this analysis, we still detect no differences.

As a third way to increase statistical power, we analyzed a class of sites that is much larger than the class of coding substitutions so that we can make measurements with much smaller standard errors; this is the class of sites affected by biased gene conversion (BGC). BGC is a selection-like process in which DNA repair acting on heterozygous sites in gene conversion tracts favors GC over AT alleles²¹. Since BGC only acts on heterozygous sites, it occurs at a rate proportional to heterozygosity, or $2p(1-p)$ for a mutation of frequency p , exactly mimicking additive selection²¹. We find that $R'_{West\ Africans/Europeans}^{GC \rightarrow AT} = 0.995 \pm 0.002$ and $R'_{West\ Africans/Europeans}^{AT \rightarrow GC} = 1.000 \pm 0.002$ by using an $R'_{X/Y}^{class1 \rightarrow class2} = R_{X/Y}^{class1 \rightarrow class2} / (R_{X/Y}^{A \leftrightarrow T} + R_{X/Y}^{C \leftrightarrow G})$ statistic that normalizes by the rate of A \leftrightarrow T and C \leftrightarrow G substitutions not expected to be affected by BGC. A further advantage of this normalization is that it also corrects for possible differences in mutation rates across lineages. For diverse population comparisons, we detect no differences significant at $|Z| > 3$ standard errors from zero with the exception of San Bushmen who have about 1% more GC \rightarrow AT mutations than other humans (significant at up to 8 standard errors) (Table S6). This is the first direct detection of less effective removal of mutations in some present-day humans than in others, and is consistent with the San being amongst the most deeply diverged human populations, which may have provided more opportunity for slight differences in the effectiveness of removal of mutations across populations to have a cumulatively measurable effect²².

To demonstrate empirically that differences in the accumulation of non-synonymous sites can be empirically detected given a sufficiently ancient population divergence time and sufficiently different subsequent demographic histories, we also analyzed two deeply sequenced genomes from archaic humans: Denisovan and Neanderthal. The ancestors of both are inferred to have maintained relatively small effective population sizes for on the order of a half million years since their main separation from present-day humans, consistent their levels of genetic diversity being 3-6 times smaller¹². A challenge in comparing the accumulation of mutations in present-day human samples to ancient samples is that fewer mutations are expected to have occurred on the lineage of ancient samples because they are from individuals who lived closer in time to the common ancestor. To correct for this, we divide the accumulation of non-synonymous mutations on each lineage by the synonymous sites: $R'_{X/Y}(non-synonymous\ class) = R_{X/Y}(non-synonymous\ class) / R_{X/Y}(synonymous)$. After removing C \rightarrow T and G \rightarrow A mutations in the archaic genomes that

have evidence of degradation leading to ancient DNA errors, we find that present-day humans have accumulated deleterious mutations at a significantly lower rate than Denisovans since separation: $R'_{Modern/Denisova}(non-synonymous) = 0.872 \pm 0.034$ ($P=0.0002$) (Table S7)¹². In contrast, $R'_{Modern/Neanderthal}(non-synonymous) = 1.037 \pm 0.037$ is consistent with 1, suggesting that deleterious mutations have not been removed as effectively on the Neanderthal as on the Denisovan lineage (Table S7). The higher resolution BGC analysis further detects that the effectiveness of removal of mutations on the Neanderthal lineage was intermediate between that of Denisovans and modern humans: $R'^{GC \rightarrow AT}_{Yoruba/Denisova} = 0.925 \pm 0.004$, $R'^{GC \rightarrow AT}_{Yoruba/Neandertal} = 0.961 \pm 0.003$, and $R'^{GC \rightarrow AT}_{Denisova/Neandertal} = 1.041 \pm 0.005$. The different rates of accumulation in Neanderthals and Denisovans despite similar inferred demographic histories (Figure 1) suggests that fitted models of demographic history, e.g. for West Africans and Europeans, may not always provide accurate predictions of the relative effectiveness of removal of mutations.

In light of these results, is there any reason to believe that weakly deleterious mutations have been removed less effectively in Europeans than in West Africans? The strongest previous evidence for such an effect was based on an alternative statistic: the proportion of polymorphic sites in the exome that are non-synonymous⁵. We therefore carried out simulations of demographic history that allowed us to study the change in this statistic over time; our simulations agree with previous simulations of the same statistic⁵, but allow for additional insights into the evolutionary forces responsible for the dynamics (Figure 2). In the first set of simulations, we adjusted the selection coefficient s in Europeans in each generation so that the quantity governing the effectiveness of selection Ns was by construction always the same in Europeans and West Africans. The simulations show that the proportion of non-synonymous sites in Europeans in fact rises more, not less, when we adjust our simulations in this way to eliminate any differences in the effectiveness of selection (blue curves in Figure 2B). Thus, the observed rise in the proportion of non-synonymous sites in Europeans is not due to differences in the effectiveness of selection after the population split, but occurs in spite of such differences. In the second set of simulations, we partitioned the change in the proportion of non-synonymous sites over time into selection and neutral effects. The simulations show that the dynamics of the previously studied statistic are driven by neutral forces (correlation coefficient of $\rho = 0.96$ to 0.99). In contrast, changes in the effectiveness with which selection removes deleterious alleles

in Europeans compared with West Africans has an effect that is opposite to the observed change ($\rho = -0.45$ to -0.27) (Figure 2C and Figure 2D). Intuitively, prior to the West African / European split, allele frequencies of non-synonymous polymorphisms would, on average, have been much lower due to the depletion of non-synonymous sites by selection, and the per-site density of non-synonymous segregating sites would also have been lower. The population entering the bottleneck primarily loses rare alleles, so the non-synonymous site allele frequency distribution would be expected to adjust faster than that for synonymous sites. Once the population re-expands, the allele frequency distribution for non-synonymous sites also adjusts faster, in this case because the same flux of new mutations into both classes causes a faster rate of replenishment of non-synonymous sites than synonymous sites due to an initially lower density. These findings illustrate the complexity of the interactions between selection and demographic history in their effects on genetic variation, and highlight an opportunity first identified by ref. ⁵, which is that joint analyses of demographic history and natural selection can provide more insight into the nature of both evolutionary forces than either type of analysis alone.

It is tempting to interpret the indistinguishable accumulations of deleterious mutations across present-day humans as implying that the overall genetic burden of disease should be similar for diverse humans. To the extent that mutations act additively this is correct, and it implies that the complex demographic events of the past are not expected to lead to substantial population differences in prevalence rates of complex disease that have an additive genetic architecture¹⁸. However, recessively or epistatically acting mutations work in combination to contribute to disease risk, and since demographic history affects allele frequencies, it affects the rate of co-occurrence of alleles. For example, Table 1 and Table S8 show that the absolute count of alleles occurring in homozygous form is empirically higher in non-Africans than in Africans for all functional site classes, confirming previous findings⁵. Thus, the relative risk for diseases that are contributed to by recessively acting mutations could be expected to be influenced by demography, as indeed is known to be the case for populations that experienced recent founder events like Ashkenazi Jews and Finns. An important direction for future work is to determine the extent to which mutations contributing to phenotypes act non-additively, as this will determine the extent to which demographic history is important in affecting human disease risk.

Methods

Data

The datasets we analyzed were published previously and are summarized here.

“*Celera*”: PCR amplification and Sanger sequencing was performed on 15 African American (AA) and 20 European American (EA) samples over the coding sequences of 10,150 genes. We downloaded ancestral and derived allele counts for 39,440 autosomal SNPs from the supplementary materials of the original study, restricting to sites with genotypes available from both AA and EA⁵.

“*1000 Genomes (1KG)*”: A total of 1,089 samples from 14 populations were analyzed in Phase 1 of the 1000 Genomes project. Illumina-based exome sequencing¹¹ was performed to ~100× average coverage after solution hybrid capture of the exome²³.

“*ESP*”: A total of 1,088 African Americans and 1,351 European Americans were sequenced as part of the National Heart, Lung and Blood Institute Exome Sequencing Project. Illumina-based exome sequencing was performed to ~100× average coverage after solution hybrid capture of the exome⁶.

“*24 Genomes*”: This dataset includes 2 samples each from 6 non-African and 5 sub-Saharan African genomes, an archaic human from Denisova Cave in Siberia sequenced to 30× coverage, and an archaic Neanderthal from Denisova Cave in Siberia sequenced to 52× coverage. All sequencing data is based on Illumina technology. We used the version of this dataset reported in ref.¹³. We only analyzed sites with genotype quality scores (GQ) of ≥ 45 ²⁴.

Mutation annotation

We annotated coding mutations using ANNOVAR²⁵, which classifies sites as “non-synonymous”, “synonymous”, “stop-gain” or “stop-loss”. We sub-classified variants using a simplified version of PolyPhen-2 that is independent of the ancestral/derived status of the human genome reference sequence (“human-free Polyphen-2”). To guarantee independence of PolyPhen-2 predictions from the human genome reference sequence, we created a simplified version that relies solely on the multi-species conservation score used in this method²⁶. This score reflects the likelihood of observing a given amino acid at a site conditional on the observed pattern of amino acid changes in the phylogeny, and is the most informative feature of PolyPhen-

2. The predictions in our simplified PolyPhen-2 method are based on the absolute values of the difference of the scores for the two alleles. By construction, this is symmetric with respect to reference/non-reference (and also ancestral/derived, major/minor) allele status. This procedure is similar to the original version of PolyPhen, but relies on the PolyPhen-2 homology search and alignment pipeline.

Statistics

We are interested in the expected number of mutations in a randomly sampled haploid exome from one population that are not seen in a randomly sampled comparison exome from another population. To compute this in a situation where we have many exomes available from each population, we do not wish to literally randomly choose an exome from each population as this would throw away data decreasing the precision of our estimates. Instead, we obtain the expected value if we performed an infinite number of random samplings. To compute this, at each variable site i in the genome we define d_A^i as the count of the mutant allele at that site in a sample of n_A^i exomes from population A and d_B^i as the count of the mutant allele in a sample of n_B^i exomes from population B. The expectations are obtained by summing over all sites in the genome.

$$L_{A \text{ not } B} = \sum_i (d_A^i / n_A^i) (1 - d_B^i / n_B^i)$$

For some analyses, we also wished to compute the relative probability that a population is homozygous for a derived allele whereas the other is not. Thus, we defined two additional statistics, now imposing a correction for limited sample size (since we need to sample two alleles from each population, we need to sample without replacement):

$$L_{A \text{ not } B}^2 = \sum_i \frac{d_A^i (1 - d_A^i)}{n_A^i (n_A^i - 1)} \left(1 - \frac{d_B^i (1 - d_B^i)}{n_B^i (n_B^i - 1)} \right)$$

We then defined the ratio statistics

$$R_{X/Y} = L_{X \text{ not } Y} / L_{Y \text{ not } X}$$

$$R_{X/Y}^2 = L_{X \text{ not } Y}^2 / L_{Y \text{ not } X}^2$$

Weighted block jackknife to estimate standard errors

We obtained standard errors using a weighted block jackknife¹⁰. We divided the SNP datasets into 100 contiguous blocks and then recomputed the statistic on all the data except for the data from that block. The variation can be converted to a standard error using jackknife theory. We assess significance based on the number of standard errors from the null expectation of $R=1$, and compute a P-value using a Z-score assuming a normal distribution.

Time-stratified computation of relative accumulation of deleterious mutation

We began with data from 10 experimentally phased genomes, all processed in a nearly identical way¹³. These genomes consisted of one each from the populations in Table 2 except for the Dinka. We then combined haploid genomes from one of 4 African and one of 6 non-African individual to make $96 = (2 \times 4) \times (2 \times 6)$ pseudo-diploid individuals. We masked the data from the exome, and ran the Pairwise Sequential Markovian Analysis (PSMC)² on the data to estimate the time since the most recent common ancestor of the two phased genomes at each location in the genome. We stratified the data into three subsets of inferred time depth, and then computed the $R_{\text{African/non-African}}$ -statistic within each time-stratified subset (using exomic sites that had been masked from the PSMC analysis so we could independently use them for analysis).

Analysis of sites susceptible to biased gene conversion (BGC)

We computed the accumulation of mutations susceptible to BGC for three different classes: GC→AT mimicking negative additive selection, AT→GC mimicking positive additive selection, and A/T or G/C polymorphisms which we treat as neutral (and use as the denominator of R'_{XY}). For BGC analyses we use the entire genome, after excluding sites in the exome. For analyses involving ancient samples, we exclude C→T and G→A sites from the analysis of GC→AT substitutions (we restrict to C→A and G→T substitutions), to avoid the degradation errors typical of ancient DNA that we are concerned may affect even the consensus genome sequences.

R'_{XY} -statistic: Correcting for branch shortening and differences in mutation rates

For analyses involving the archaic Denisovan and Neanderthal samples, which are many tens of thousands of years old and thus have experienced less evolution from the common ancestor than

present-day humans to which they are compared, we do not expect that $L_{archaic\ not\ modern} = L_{modern\ not\ archaic}$ even for neutral sites. For all analyses involving ancient samples, we instead compute normalized statistics $L_{A\ not\ B}'$ and $L_{B\ not\ A}'$, where we divide both $L_{A\ not\ B}$ and $L_{B\ not\ A}$ by the accumulation of mutations at sites that are expected to act neutrally (synonymous sites for coding sequences and A/T + C/G for BGC). Thus, $L_{A\ not\ B}'^{class} = L_{A\ not\ B}^{class} / L_{A\ not\ B}^{normalization}$. We then define:

$$R_{X/Y}'^{class} = (L_{X\ not\ Y}^{class} / L_{Y\ not\ X}^{class}) / (L_{X\ not\ Y}^{normalization} / L_{Y\ not\ X}^{normalization}) = R_{X/Y}^{class} / R_{X/Y}^{normalization}$$

This $R_{X/Y}'$ -statistic not only corrects for branch shortening in the ancient samples, but also has the benefit of correcting for any differences in mutation rate that might have arisen on one lineage or another since population separation.

Simulations

We wrote a forward simulation in C that implements an infinite sites model. Each mutation is assumed to occur at an unlinked site. To the extent that linkage affects the expected values of the statistics we compute, our simulations are not capturing these effects.

There is an initial burn-in period of 250,000 generations to generate an equilibrium allele frequency spectrum. The simulator samples the allele counts in the current generation based on the frequencies in the previous generation, the selection coefficient s , the dominance coefficient h (usually set to additive or $h=0.5$), and the current population size.

For modeling West African and European history in the simulations reported in the main text, we use a demographic model previously fitted to genetic data⁶. (Figure S1 reports results for other four different demographic histories, shown in Table S9). For comparisons of West African and archaic population history we also use a previously fitted demographic model¹³. We use a mutation rate of 2×10^{-8} /base pair/generation.

For analyses of the proportion of sites that are expected to be non-synonymous in a sample size of 40 chromosomes, we use a hypergeometric distribution to obtain the expected value of this statistic. If the population size in a generation is N and K_i is the number of copies of the derived allele at site i , then we can compute the probability that a sample of 40 chromosomes is polymorphic at a site as 1 minus the hypergeometric probability of 0 or 40 derived alleles:

$$Probability\ that\ site\ i\ is\ segregating = 1 - \frac{\binom{K_i}{0}\binom{N-K_i}{40}}{\binom{N}{40}} - \frac{\binom{K_i}{0}\binom{N-K_i}{0}}{\binom{N}{40}}$$

We average this probability over all simulated positions to obtain the density of segregating sites.

Integrating over distributions of selection coefficients

For some statistics, we wished to obtain an expected value integrating over distributions of selection coefficients. To achieve this, we carried out simulation series for different selection coefficients; for example, for Figure 2, each of 19 values: $s = \{-1 \times 10^6, -2 \times 10^6, -5 \times 10^6, -1 \times 10^5, -2 \times 10^5, -5 \times 10^5, -1 \times 10^4, -2 \times 10^4, -5 \times 10^4, -1 \times 10^3, -2 \times 10^3, -5 \times 10^3, -0.01, -0.02, -0.05, -0.1, -0.2, -0.5, -1\}$. To compute expected values for $L_{X\ not\ Y}$, $L_{Y\ not\ X}$, and the density of segregating sites per base pair in a fixed sample size of 40 chromosomes, we use a weighted average of the values of the simulated single selection coefficient statistics. For some analyses, we use the distribution of human selection coefficients for non-synonymous sites from ref. ¹⁷, where the probability of a given value of $-s$ is drawn from a gamma distribution fitted to European genetic data with $\alpha=0.206$ and $\beta=15400$. For analyses of the expected value of $R_{WestAfrica/Europe}$ stratified by PolyPhen-2 functional class, we use the values inferred in Note S1.

Simulations forcing the effectiveness of selection in Europeans and West Africans to be the same

To evaluate whether differences in the effectiveness of selection in the Europeans and West African populations since their split could be explaining the observed rise in the proportion of non-synonymous sites in Europeans above baseline, we modified the simulator so that in every generation i , the selection coefficient in Europeans $s_{e,i}$ is determined dynamically. Define $N_{e,i}$ and $N_{a,i}$ as the diploid population sizes in Europeans and Africans, respectively, and define the selection coefficient in Africans (held constant) as $s_{a,i}$. We then set the selection coefficient in Europeans in each generation to be $s_{e,i} = s_{a,i}(N_{a,i}/N_{e,i})$. This procedure has the consequence that $N_{e,i}s_{e,i} = N_{e,i}s_{a,i}(N_{a,i}/N_{e,i}) = N_{a,i}s_{a,i}$. Since the quantity Ns governs the effectiveness of selection, selection is guaranteed to be equally effective in both populations at all times.

Partitioning the evolutionary dynamics into the effects of selection and neutral effects

We modified the simulation to sample two counts of derived alleles in each generation for a given selection coefficient s and nucleotide position i . The first count is $A_{s,i}$, which reflects the forces of selection, mutation, and stochastic sampling. The second is $N_{s,i}$, which reflects the effects of mutation and stochastic sampling but not selection. The counts in each generation are only updated based on $A_{s,i-1}$ in the previous generation, so the long-term evolutionary trajectory properly incorporates the effects of natural selection as they have accumulated over generations.

We average the values of $N_{s,i}$ and $A_{s,i}$ over simulation replicates, and compute a weighted average of the results based on the distribution of selection coefficients from ref. ¹⁷. We define the proportion of sites that are expected to be non-synonymous in a given generation as $PropAll_i = A_{s,i}/(A_{s,i} + A_{0,i})$, and the proportion that would be non-synonymous if selection had been switched off in that generation as $PropNeu_i = N_{s,i}/(N_{s,i} + A_{0,i})$.

With this notation, the expected change in the proportion of nonsynonymous sites due to all evolutionary forces in generation i is $\delta PropAll_i = PropAll_i - PropAll_{i-1}$. The proportion due to neutral forces only is $\delta PropNeu_i = PropNeu_i - PropAll_{i-1}$, and the proportion due to selective forces only is $\delta PropSel_i = PropAll_i - PropNeu_i$.

To compare the effect of an evolutionary force in a given generation to what it was in the ancestral population prior to the split (>2,040 generations ago in the simulations of Figure 2), we defined the baseline-corrected statistics $\Delta PropSel_i = \delta PropSel_i - \delta PropSel_{baseline}$, $\Delta PropNeu_i = \delta PropNeu_i - \delta PropNeu_{baseline}$, and $\Delta PropAll_i = \delta PropAll_i - \delta PropAll_{baseline}$. These statistics are positive if the effectiveness of removal of mutations due to an evolutionary force is less than in the ancestral population, and negative if the effectiveness is greater than in the ancestral population. These are the statistics plotted in Figure 2C and integrated to obtain cumulative effects in Figure 2D.

Figure Legends

Figure 1: The effect of demographic history on the accumulation of deleterious mutations..

To study the expected value of $R_{WestAfrica/Europe}$ stratified by selection coefficient, we simulated a previously published model of the joint history of West Africans and Europeans⁶, for a range of selection coefficients, assuming an additive model of nature selection (Figure S1 shows similar results for other demographic models). The simulations show that $R_{WestAfrica/Europe}$ dips below a potentially detectable ratio of 0.95 for $s \in (-0.0004, -0.004)$. We also simulated a published model of the history of archaic Denisovans, archaic Neanderthals, and West Africans¹³. The simulations predicts similar curves for $R'_{WestAfrica/Denisova}$ and $R'_{WestAfrica/Neanderthal}$ reflecting their similar inferred demographic histories (we use a normalized R' statistic to correct for the effects of branch shortening in these ancient lineages). The simulations show that $R'_{WestAfrica/Denisova}$ is expected to below a detectable ratio of 0.95 for $s \in (-0.00002, -0.03)$ and that $R'_{WestAfrica/Neanderthal}$ is expected to be below 0.95 for $s \in (-0.00002, -0.09)$.

Figure 2: The rise in the proportion of non-synonymous sites in Europeans compared with West Africans is not due to a reduced effectiveness of selection in Europeans since the split.

(A) The West African and European diploid population sizes for the two simulated models, both of which specify a population split 2,040 generations ago. The plots of the temporal dynamics of the statistics in subsequent panels are restricted to the European population, as the West African population size does not fluctuate enough to result in appreciable changes from the baseline. (B) We show the values of key statistics as a fraction of the baseline. The present-day proportion of non-synonymous sites in Europeans is higher than in the ancestral populations (black curves). This cannot be attributed to less effective removal of deleterious mutations in Europeans than in Africans since the population split, as we can see from the fact that when we carry out simulations in which the selection coefficient in Europeans per generation is set so that the effectiveness of selection Ns in the two populations is the same, the rise actually becomes greater (blue curves). (C) Partitioning of the change in the proportion of non-synonymous sites per generation into neutral and selective forces shows that for the West African / European

comparison, the temporal dynamics are driven by neutral forces (strong positive correlation in the dynamics) and not by the selective forces (negative correlation). (D) Plots of the cumulative effect of each evolutionary force compared to baseline show that differences in the effectiveness of selection between Europeans and West Africans since they separated in fact have a net negative, not a net positive effect on the proportion of non-synonymous sites in Europeans.

Table 1: Accumulation of different classes of mutation in exomes of West African compared to exomes of European ancestry

Data set	West Africans	Europeans	<i>R</i> : Relative rate of lineage specific mutations					<i>R</i> ² : Relative rate of homozygosity for lineage specific mutations				
			<i>R</i> (synonymous)	<i>R</i> (All non-synonymous)	<i>R</i> (Benign)	<i>R</i> (Possibly damaging)	<i>R</i> (Probably damaging)	<i>R</i> ² (synonymous)	<i>R</i> ² (All non-synonymous)	<i>R</i> ² (Benign)	<i>R</i> ² (Possibly damaging)	<i>R</i> ² (Probably damaging)
24 deep genomes	4	4	1.022 (0.012)	1.008 (0.015)	1.002 (0.018)	1.007 (0.040)	1.031 (0.038)	0.652 (0.014)	0.629 (0.019)	0.628 (0.021)	0.602 (0.043)	0.660 (0.047)
Celera exomes	15	20	0.982 (0.011)	1.010 (0.019)	1.011 (0.022)	1.019 (0.043)	0.992 (0.039)	0.610 (0.011)	0.586 (0.047)	0.583 (0.021)	0.616 (0.053)	0.586 (0.047)
1KG exomes	88	85	1.019 (0.010)	0.994 (0.012)	0.999 (0.015)	0.955 (0.028)	1.011 (0.026)	0.655 (0.012)	0.656 (0.014)	0.639 (0.018)	0.599 (0.032)	0.642 (0.032)
ESP exomes	1,088	1,351	1.004 (0.009)	1.001 (0.011)	0.993 (0.013)	1.001 (0.021)	1.037 (0.029)	0.605 (0.010)	0.608 (0.011)	0.598 (0.015)	0.578 (0.025)	0.630 (0.034)

Notes: ± 1 standard errors are obtained from a Block Jackknife with 100 equally sized blocks. For the whole genomes, Yoruba+Mandenka represent West Africans, and French+Sardinian represent Europeans. For the 1000 Genomes Data (1KG), YRI represent West Africans and CEU Europeans. The results for the Celera and ESP analyses represent people of West African ancestry using African Americans.

Table 2: R_{XY} (probably damaging) for all pairs of deep genome populations (bottom left) and 1000 Genomes populations (top right)

			IBS (Spanish)	GBR (British)	FIN (Finns)	CEU (European)	JPT (Japanese)	CHS (Chinese)	CHB (Chinese)	PUR (Puerto Rican)	MXL (Mexican)	CLM (Columbian)	YRI (Nigerian)	LWK (Kenyan)	ASW (African American)	IKG
		TSI (98)	1.025 (0.013)	1.004 (0.007)	1.030 (0.009)	1.012 (0.007)	1.014 (0.025)	1.029 (0.025)	1.024 (0.025)	1.026 (0.009)	1.042 (0.018)	1.022 (0.012)	0.998 (0.026)	0.981 (0.024)	1.008 (0.021)	TSI
		IBS (14)		0.979 (0.013)	1.005 (0.014)	0.987 (0.013)	0.991 (0.028)	1.006 (0.028)	1.001 (0.028)	1.002 (0.014)	1.018 (0.022)	0.998 (0.016)	0.978 (0.026)	0.962 (0.025)	0.987 (0.021)	IBS
	Denisova (1)			GBR (89)	1.026 (0.008)	1.008 (0.007)	1.010 (0.026)	1.026 (0.026)	1.021 (0.026)	1.023 (0.01)	1.039 (0.019)	1.018 (0.013)	0.995 (0.027)	0.978 (0.025)	1.005 (0.022)	GBR
Neanderthal	0.695 (0.046)	Neanderthal(1)			FIN (93)	0.983 (0.008)	0.986 (0.024)	1.001 (0.025)	0.996 (0.025)	0.998 (0.011)	1.014 (0.017)	0.993 (0.012)	0.975 (0.026)	0.958 (0.024)	0.984 (0.021)	FIN
Dinka	0.724 (0.037)	0.979 (0.058)	Dinka (2)			CEU (85)	1.002 (0.025)	1.018 (0.025)	1.013 (0.025)	1.015 (0.01)	1.030 (0.018)	1.010 (0.013)	0.988 (0.026)	0.971 (0.024)	0.998 (0.021)	CEU
Mandenka	0.734 (0.036)	1.004 (0.055)	1.029 (0.0442)	Mandenka (2)			JPT (89)	1.017 (0.009)	1.012 (0.009)	1.011 (0.023)	1.028 (0.02)	1.007 (0.022)	0.986 (0.028)	0.969 (0.026)	0.995 (0.024)	JPT
Mbuti	0.734 (0.034)	1.014 (0.048)	1.041 (0.041)	1.026 (0.04)	Mbuti (2)			CHS (100)	0.994 (0.007)	0.996 (0.022)	1.012 (0.02)	0.991 (0.021)	0.973 (0.028)	0.957 (0.026)	0.982 (0.024)	CHS
San	0.759 (0.038)	1.026 (0.056)	1.024 (0.039)	1.005 (0.04)	0.98 (0.038)	San (2)			CHB (97)	1.001 (0.022)	1.017 (0.021)	0.996 (0.021)	0.978 (0.027)	0.961 (0.026)	0.986 (0.024)	CHB
Yoruba	0.738 (0.036)	1.004 (0.057)	1.007 (0.035)	0.985 (0.039)	0.961 (0.036)	0.975 (0.036)	Yoruba (2)			PUR (55)	1.015 (0.014)	0.995 (0.008)	0.977 (0.022)	0.96 (0.021)	0.986 (0.017)	PUR
Dai	0.765 (0.038)	1.066 (0.063)	1.075 (0.046)	1.047 (0.046)	1.013 (0.044)	1.051 (0.04)	1.085 (0.041)	Dai (2)			MXL (64)	0.980 (0.012)	0.964 (0.027)	0.948 (0.026)	0.972 (0.022)	MXL
French	0.732 (0.037)	0.993 (0.060)	0.994 (0.045)	0.959 (0.044)	0.937 (0.044)	0.957 (0.04)	0.972 (0.039)	0.908 (0.039)	French (2)			CLM (60)	0.980 (0.024)	0.963 (0.023)	0.989 (0.019)	CLM
Han	0.762 (0.036)	1.078 (0.057)	1.061 (0.047)	1.048 (0.048)	1.013 (0.039)	1.043 (0.041)	1.080 (0.043)	0.984 (0.041)	1.110 (0.053)	Han (2)			YRI (88)	0.983 (0.009)	1.010 (0.009)	YRI
Karitiana	0.712 (0.041)	0.988 (0.062)	0.967 (0.047)	0.938 (0.047)	0.929 (0.045)	0.938 (0.044)	0.96 (0.044)	0.861 (0.041)	0.966 (0.046)	0.875 (0.046)	Karitiana (2)			LWK (96)	1.027 (0.011)	LWK
Papuan	0.726 (0.038)	1.008 (0.063)	1.006 (0.052)	0.974 (0.046)	0.964 (0.044)	0.979 (0.044)	0.995 (0.048)	0.924 (0.041)	1.020 (0.048)	0.911 (0.042)	1.046 (0.053)	Papuan (2)			ASW (61)	
Sardinian	0.750 (0.039)	1.001 (0.057)	1.020 (0.046)	0.969 (0.043)	0.958 (0.038)	0.969 (0.043)	0.988 (0.044)	0.919 (0.041)	1.014 (0.045)	0.917 (0.040)	1.052 (0.055)	1.008 (0.048)	Sardinian (2)			
Deep genomes	Denisova	Neanderthal	Dinka	Mandenka	Mbuti	San	Yoruba	Dai	French	Han	Karitiana	Papuan				

Notes: ± 1 standard errors (parentheses) are based on a Block Jackknife with 100 equally sized blocks. We highlight numbers > 4 standard errors from expectation. Ratios for Neanderthal and Denisova are normalized by the number of synonymous sites on each lineage, to adjust for the expectation of fewer mutations in the ancient samples than in the present-day human samples due to less time elapsed since divergence (all other comparisons are un-normalized). Ratios are based on the accumulation observed in the population in the row divided by that in the population in the column. Numbers in parentheses are sample sizes.

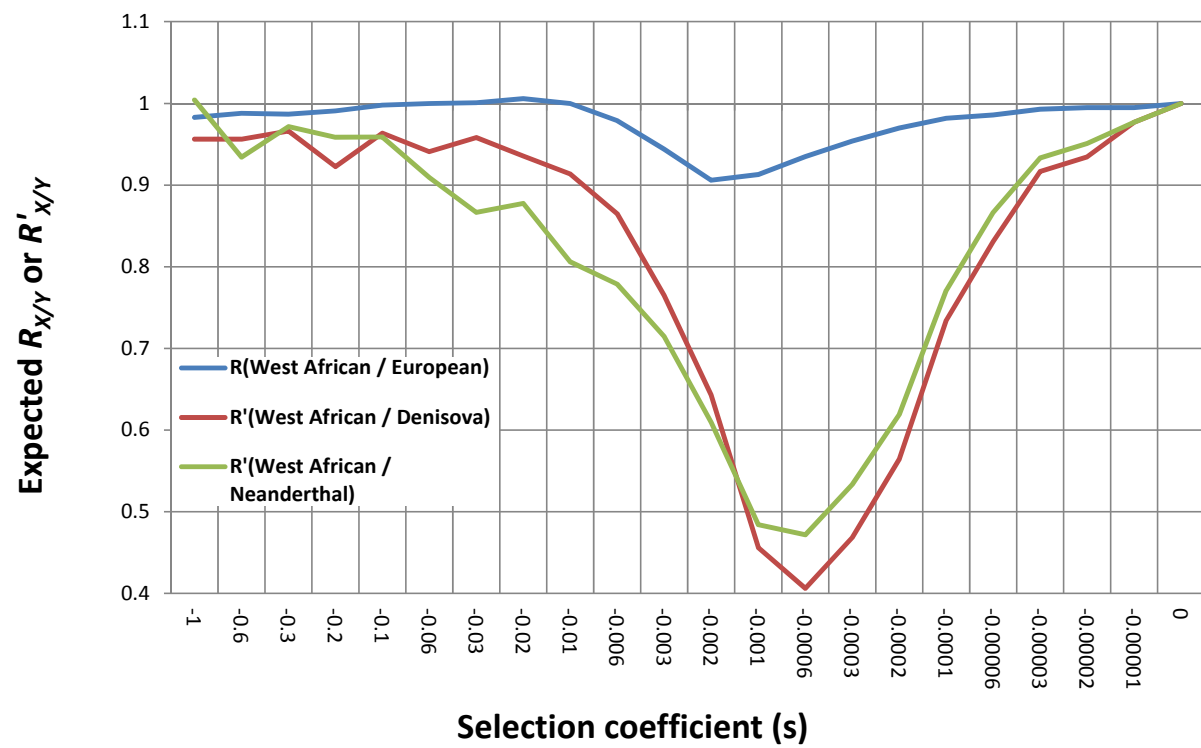
Acknowledgments

We are grateful to Joshua Akey, David Altshuler, Carlos Bustamante, Sergi Castellano, Cesare de Filippo, Alexey Kondrashov, Eric Lander, Kirk Lohmueller Swapan Mallick, Svante Pääbo, Nick Patterson, Jonathan Pritchard, Joshua Schaiber, Guy Sella and Montgomery Slatkin, for valuable discussions. D.R. was supported by NIH grants GM100233 and HG006399 and by NSF grant 1032255. S.S. was supported by NIH grants R01GM078598 and R01MH101244. R.D was supported by a Banting fellowship from the Canadian Institutes of Health Research.

References

1. Charlesworth, B. Fundamental concepts in genetics: effective population size and patterns of molecular evolution and variation. *Nat Rev Genet* 10, 195-205 (2009).
2. Li, H. & Durbin, R. Inference of human population history from individual whole-genome sequences. *Nature* 475, 493-6 (2011).
3. Keinan, A., Mullikin, J.C., Patterson, N. & Reich, D. Measurement of the human allele frequency spectrum demonstrates greater genetic drift in East Asians than in Europeans. *Nat Genet* 39, 1251-5 (2007).
4. Gronau, I., Hubisz, M.J., Gulko, B., Danko, C.G. & Siepel, A. Bayesian inference of ancient human demography from individual genome sequences. *Nat Genet* 43, 1031-4 (2011).
5. Lohmueller, K.E. *et al.* Proportionally more deleterious genetic variation in European than in African populations. *Nature* 451, 994-7 (2008).
6. Tennessen, J.A. *et al.* Evolution and functional impact of rare coding variation from deep sequencing of human exomes. *Science* 337, 64-9 (2012).
7. Fu, W. *et al.* Analysis of 6,515 exomes reveals the recent origin of most human protein-coding variants. *Nature* 493, 216-20 (2013).
8. Casals, F. *et al.* Whole-exome sequencing reveals a rapid change in the frequency of rare functional variants in a founding population of humans. *PLoS Genet* 9, e1003815 (2013).
9. Kidd, J.M. *et al.* Population genetic inference from personal genome data: impact of ancestry and admixture on human genomic variation. *Am J Hum Genet* 91, 660-71 (2012).
10. Kunsch, H.R. The Jackknife and the Bootstrap for General Stationary Observations. *Annals of Statistics* 17, 1217-1241 (1989).
11. Abecasis, G.R. *et al.* An integrated map of genetic variation from 1,092 human genomes. *Nature* 491, 56-65 (2012).
12. Meyer, M. *et al.* A high-coverage genome sequence from an archaic Denisovan individual. *Science* 338, 222-6 (2012).
13. Prufer, K. *et al.* The complete genome sequence of a Neanderthal from the Altai Mountains. *Nature* 505, 43-9 (2014).
14. Turchin, M.C. *et al.* Evidence of widespread selection on standing variation in Europe at height-associated SNPs. *Nat Genet* 44, 1015-9 (2012).
15. Gravel, S. *et al.* Demographic history and rare allele sharing among human populations. *Proc Natl Acad Sci U S A* 108, 11983-8 (2011).
16. Balick, D.J., Do, R., Reich, D. & Sunyaev, S.R. Response to a population bottleneck can be used to infer recessive selection. *Submitted. arXiv. 1312.3028.*
17. Boyko, A.R. *et al.* Assessing the evolutionary impact of amino acid mutations in the human genome. *PLoS Genet* 4, e1000083 (2008).
18. Simons, Y.B., Turchin, M.C., Pritchard, J.K. & Sella, G. The deleterious mutation load is insensitive to recent population history. *Nat Genet* (2014).

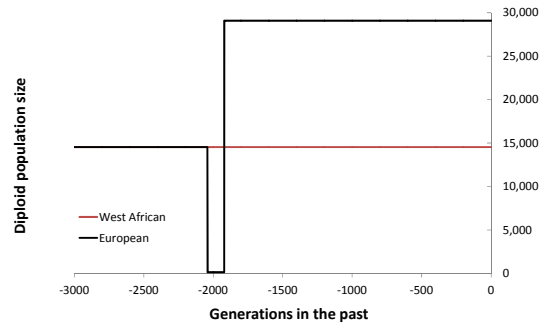
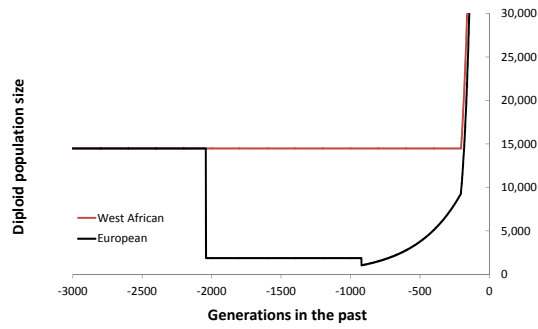
19. Adzhubei, I., Jordan, D.M. & Sunyaev, S.R. Predicting functional effect of human missense mutations using PolyPhen-2. *Curr Protoc Hum Genet* Chapter 7, Unit7 20 (2013).
20. Ng, P.C. & Henikoff, S. Predicting deleterious amino acid substitutions. *Genome Res* 11, 863-74 (2001).
21. Duret, L. & Galtier, N. Biased gene conversion and the evolution of mammalian genomic landscapes. *Annu Rev Genomics Hum Genet* 10, 285-311 (2009).
22. Schuster, S.C. *et al.* Complete Khoisan and Bantu genomes from southern Africa. *Nature* 463, 943-7 (2010).
23. Gnirke, A. *et al.* Solution hybrid selection with ultra-long oligonucleotides for massively parallel targeted sequencing. *Nat Biotechnol* 27, 182-9 (2009).
24. Reich, D. Insights into human population history from a high coverage Neandertal genome. *Society for Molecular Biology and Evolution 2013 Meeting*. Abstract 37(2013).
25. Wang, K., Li, M. & Hakonarson, H. ANNOVAR: functional annotation of genetic variants from high-throughput sequencing data. *Nucleic Acids Res* 38, e164 (2010).
26. Sunyaev, S.R. *et al.* PSIC: profile extraction from sequence alignments with position-specific counts of independent observations. *Protein Eng* 12, 387-94 (1999).



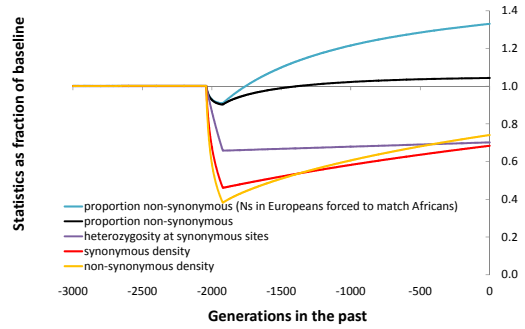
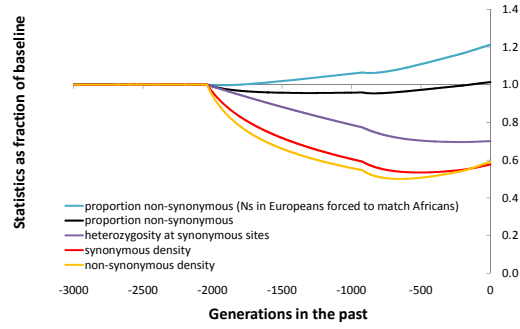
Tennessen et al.

Bottleneck and growth

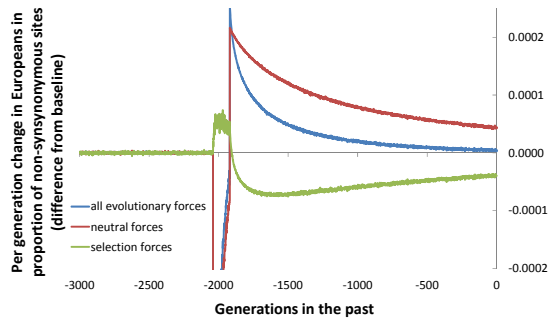
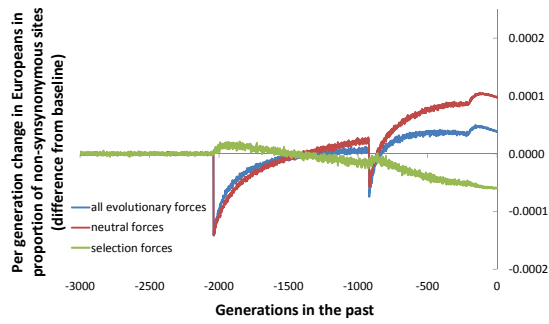
A



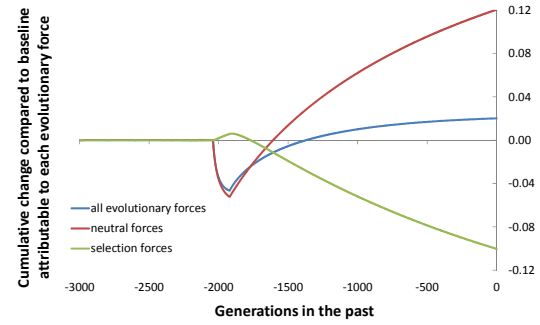
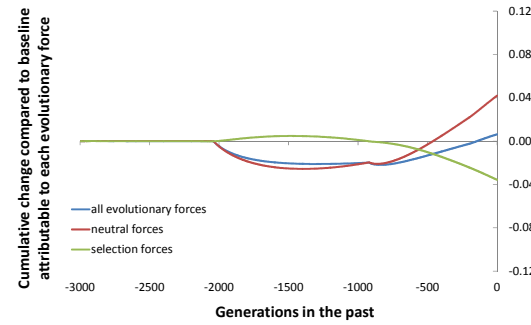
B



C



D



Supplementary Materials

No evidence that natural selection has been less effective at removing deleterious mutations in non-Africans than in West Africans

Table of contents	1
Table S1 – Sample sizes in each dataset	2
Table S2 – Version of Table 1 for sites with a consistent allele among great apes	3
Table S3 – Expansion of Table 2 into PolyPhen-2 classes	4-8
Table S4 – Expected $R_{WestAfrica/Europe}$ for different models of demography	9
Table S5 – $R_{African/Non-African}$-statistic stratified by time depth of comparison	10
Table S6 – Biased Gene Conversion analysis for all population pairs	11-12
Table S7 – Key statistics as a function of allelic substitution patterns	13
Table S8 – R^2_{XY}-statistic for all population pairs	14
Table S9 – Parameters of simulated demographic models	15
Figure S1 – $R_{WestAfrica/Europe}$ for four demographic histories (simulations)	16
Supplementary References for Tables and Figures	17
Note S1 – Inferred distributions of selection coefficients for PolyPhen-2 classes	18-27
Note S2 – Proportion of non-synonymous sites is driven by neutral demography	28-31

Table S1: Sample sizes in each dataset

Dataset	Population	N
24 diverse genomes ¹	Denisova	1
	Neanderthal	1
	Mbuti	2
	San	2
	Mandenka	2
	Yoruba	2
	Dinka	2
	Papuan	2
	Sardinian	2
	Dai	2
	Karitiana	2
	Han	2
	French	2
Lohmueller ²	African American	15
	European American	20
1000 Genomes ³	ASW	61
	CEU	85
	CHB	97
	CHS	100
	CLM	60
	FIN	93
	GBR	89
	IBS	14
	JPT	89
	LWK	96
	MXL	64
	PUR	55
	TSI	98
	YRI	88
Exome Sequencing Project ⁴	African American	1,088
	European American	1,351

ASW: African Ancestry in Southwest US; CEU: Utah residents (CEPH) with Northern and Western European ancestry; CHB: Han Chinese in Beijing, China; CHS: Han Chinese South; CLM: Colombian in Medellin, Colombia; FIN: Finnish from Finland; GBR: British from England and Scotland (GBR); IBS: Iberian populations in Spain; JPT: Japanese in Tokyo, Japan; LWK: Luhya in Webuye, Kenya; MXL: Mexican Ancestry in Los Angeles, CA; MXL: Mexican Ancestry in Los Angeles, CA; PUR: Puerto Rican in Puerto Rico; TSI: Toscani in Italia; YRI: Yoruba in Ibadan, Nigeria.

Table S2: Version of Table 1 for sites with a consistent allele among great apes

Data set	West Africans	Europeans	<i>R</i> : Relative rate of lineage specific mutations					<i>R</i> ² : Relative rate of homozygosity for lineage specific mutations				
			<i>R</i> _(synonymous)	<i>R</i> _(All non-synonymous)	<i>R</i> _(Benign)	<i>R</i> _(Possibly damaging)	<i>R</i> _(Probably damaging)	<i>R</i> ² _(synonymous)	<i>R</i> ² _(All non-synonymous)	<i>R</i> ² _(Benign)	<i>R</i> ² _(Possibly damaging)	<i>R</i> ² _(Probably damaging)
24 deep genomes	4	4	1.011 (0.014)	1.015 (0.015)	1.015 (0.019)	0.991 (0.039)	1.038 (0.038)	0.628 (0.015)	0.626 (0.018)	0.630 (0.021)	0.570 (0.043)	0.661 (0.052)
Celera exomes	15	20	0.990 (0.012)	1.012 (0.020)	1.018 (0.023)	1.009 (0.044)	0.991 (0.043)	0.599 (0.011)	0.572 (0.051)	0.585 (0.024)	0.604 (0.054)	0.572 (0.051)
1KG exomes	88	85	1.001 (0.012)	0.987 (0.013)	0.992 (0.016)	0.948 (0.029)	1.003 (0.028)	0.624 (0.013)	0.616 (0.014)	0.613 (0.017)	0.575 (0.031)	0.612 (0.035)
ESP exomes	1,088	1,351	1.007 (0.011)	0.999 (0.012)	0.993 (0.014)	0.984 (0.028)	1.040 (0.030)	0.603 (0.011)	0.594 (0.014)	0.585 (0.016)	0.551 (0.025)	0.628 (0.038)

Notes: This is the same analysis as Table 1, restricting to sites where chimpanzee and at least one of gorilla and orangutan have an allele call and all of the great apes are consistent (data from the EPO six-way primate alignment). ± 1 standard errors are from a Block Jackknife with 100 equally sized blocks. For the whole genomes, Yoruba+Mandenka represent West Africans, and French+Sardinian represent Europeans. For the 1000 Genomes Data (1KG), YRI represent West Africans and CEU Europeans. The Celera and ESP datasets use African Americans to represent people with West African ancestry.

Table S3: Expansion of Table 2 into PolyPhen2 classes

Table S3A– Synonymous mutations for all pairs of 24 deep genomes (bottom left) and 1000 Genomes populations (top right)

			IBS (Spanis h)	GBR (British)	FIN (Finnish)	CEU (European)	JPT (Japanese)	CHS (Chinese)	CHB (Chinese)	PUR (Pu.Ric.)	MXL (Mexican)	CLM (Colomb.)	YRI (Nigerian)	LWK (Kenyan)	ASW (Afr. Am.)	IKG	
			TSI (98)	1.015 (0.004)	1.002 (0.003)	0.997 (0.004)	0.999 (0.003)	0.988 (0.008)	0.994 (0.009)	0.991 (0.008)	1.002 (0.003)	0.99 (0.005)	0.991 (0.004)	0.981 (0.009)	0.973 (0.008)	0.987 (0.007)	TSI (Italian)
			IBS (14)	0.987 (0.004)	0.982 (0.004)	0.984 (0.004)	0.974 (0.008)	0.98 (0.008)	0.977 (0.008)	0.988 (0.005)	0.976 (0.006)	0.976 (0.005)	0.97 (0.009)	0.962 (0.009)	0.975 (0.008)	0.985 (0.007)	IBS (Spanish)
			Denis- ova (1)	GBR (89)	0.995 (0.003)	0.997 (0.002)	0.986 (0.008)	0.992 (0.008)	0.989 (0.008)	1 (0.003)	0.988 (0.005)	0.989 (0.004)	0.979 (0.009)	0.972 (0.008)	0.985 (0.007)	0.985 (0.007)	GBR (British)
Neand- erthal	n/a	Neand- erthal(1)				FIN (93)	1.002 (0.003)	0.991 (0.008)	0.997 (0.008)	0.994 (0.008)	1.005 (0.004)	0.993 (0.005)	0.994 (0.004)	0.983 (0.009)	0.976 (0.009)	0.99 (0.007)	FIN (Finnish)
Dinka	n/a	n/a	Dinka (2)				CEU (85)	0.989 (0.008)	0.994 (0.008)	0.992 (0.008)	1.003 (0.004)	0.991 (0.005)	0.991 (0.004)	0.981 (0.009)	0.974 (0.009)	0.988 (0.008)	CEU (Eur.)
Mand- enka	n/a	n/a	1.001 (0.013)	Mand- enka (2)				JPT (89)	1.007 (0.003)	1.004 (0.003)	1.014 (0.007)	1.003 (0.007)	1.003 (0.007)	0.99 (0.01)	0.983 (0.009)	0.997 (0.009)	JPT (Japanese)
Mbuti	n/a	n/a	0.99 (0.013)	0.993 (0.012)	Mbuti (2)				CHS (100)	0.997 (0.002)	1.008 (0.008)	0.997 (0.007)	0.997 (0.007)	0.986 (0.01)	0.978 (0.01)	0.992 (0.009)	CHS (Chinese)
San	n/a	n/a	0.979 (0.014)	0.975 (0.014)	0.982 (0.014)	San (2)				CHB (97)	1.01 (0.007)	0.999 (0.007)	1 (0.007)	0.988 (0.01)	0.98 (0.009)	0.994 (0.008)	CHB (Chinese)
Yoruba	n/a	n/a	0.981 (0.013)	0.981 (0.012)	0.99 (0.011)	1.004 (0.014)	Yoruba (2)				PUR (55)	0.989 (0.004)	0.989 (0.003)	0.979 (0.008)	0.972 (0.008)	0.986 (0.007)	PUR (Pu.Ric.)
Dai	n/a	n/a	0.969 (0.015)	0.971 (0.014)	0.978 (0.014)	0.994 (0.014)	0.988 (0.013)	Dai (2)				MXL (64)	1 (0.004)	0.988 (0.009)	0.981 (0.008)	0.995 (0.008)	MXL (Mexican)
French	n/a	n/a	0.966 (0.013)	0.971 (0.014)	0.977 (0.014)	0.991 (0.014)	0.984 (0.012)	0.995 (0.016)	French (2)				CLM (60)	0.988 (0.008)	0.98 (0.008)	0.995 (0.007)	CLM (Colomb.)
Han	n/a	n/a	0.99 (0.017)	0.992 (0.014)	0.996 (0.016)	1.013 (0.015)	1.009 (0.014)	1.029 (0.015)	1.028 (0.017)	Han (2)				YRI (88)	0.992 (0.003)	1.007 (0.003)	YRI (Nigerian)
Karit- iana	n/a	n/a	0.983 (0.017)	0.983 (0.015)	0.986 (0.016)	1.001 (0.016)	0.994 (0.014)	1.012 (0.015)	1.02 (0.017)	0.987 (0.018)	Karitiana (2)				LWK (96)	1.015 (0.003)	LWK (Kenyan)
Papuan	n/a	n/a	0.958 (0.015)	0.962 (0.015)	0.97 (0.015)	0.982 (0.015)	0.977 (0.013)	0.985 (0.016)	0.991 (0.016)	0.959 (0.016)	0.97 (0.016)	Papuan (2)				ASW (61)	
Sard- inian	n/a	n/a	0.976 (0.013)	0.972 (0.015)	0.978 (0.015)	0.996 (0.013)	0.987 (0.013)	1.004 (0.015)	1.01 (0.013)	0.978 (0.014)	0.991 (0.016)	1.018 (0.015)	Sardinian (2)				
Deep genomes	Denis- ova	Neander- thal	Dinka	Mand- enka	Mbuti	San	Yoruba	Dai	French	Han	Karitiana	Papuan					

Notes: ±1 standard errors (parentheses) are based on a Block Jackknife with 100 equally sized blocks. Highlighted numbers indicate P < 0.001.

* $R_{X/Y}$ ratios involving the ancient Denisova and Neanderthal samples are not shown as fewer mutations are expected for these than modern human lineages since divergence. Ratios are based on the accumulation of mutations observed in the population in the row divided by the accumulation of mutations observed in the population in the column. The number in parentheses indicates the number of samples per population.

Table S3B– All non-synonymous mutations for all pairs of 24 deep genomes (bottom left) and 1000 Genomes populations (top right)

			IBS (Spanish)	GBR (British)	FIN (Finnish)	CEU (European)	JPT (Japanese)	CHS (Chinese)	CHB (Chinese)	PUR (Pu.Ric.)	MXL (Mexican)	CLM (Colomb.)	YRI (Nigerian)	LWK (Kenyan)	ASW (Afr.Am.)	1KG		
TSI (98)			1.026 (0.005)	1.003 (0.003)	1.003 (0.004)	1 (0.003)	0.998 (0.01)	1.005 (0.011)	1.001 (0.011)	1.017 (0.004)	1.014 (0.006)	1.004 (0.005)	1.005 (0.012)	0.992 (0.011)	1.013 (0.01)	TSI (Italian)		
			IBS (14)	0.978 (0.005)	0.977 (0.005)	0.974 (0.005)	0.974 (0.011)	0.981 (0.011)	0.978 (0.011)	0.993 (0.006)	0.989 (0.008)	0.979 (0.006)	0.986 (0.012)	0.972 (0.012)	0.992 (0.01)	IBS (Spanish)		
Denis- ova (1)			GBR (89)		0.999 (0.003)	0.996 (0.002)	0.995 (0.01)	1.002 (0.011)	0.998 (0.01)	1.014 (0.005)	1.011 (0.006)	1.001 (0.005)	1.003 (0.012)	0.989 (0.011)	1.01 (0.01)	GBR (British)		
Neand- erthal	0.875 (0.031)	Neand- erthal (1)				FIN (93)	0.997 (0.003)	0.995 (0.01)	1.003 (0.011)	0.999 (0.011)	1.015 (0.005)	1.011 (0.007)	1.001 (0.005)	1.003 (0.013)	0.99 (0.012)	1.011 (0.01)	FIN (Finnish)	
Dinka	0.862 (0.025)	0.969 (0.031)	Dinka (2)					CEU (85)	0.998 (0.011)	1.005 (0.011)	1.002 (0.011)	1.018 (0.005)	1.014 (0.007)	1.004 (0.005)	1.006 (0.013)	0.992 (0.012)	1.013 (0.01)	CEU (European)
Mand- enka	0.865 (0.023)	0.979 (0.028)	1.014 (0.017)	Mand- enka (2)				JPT (89)	1.008 (0.004)	1.004 (0.003)	1.019 (0.009)	1.016 (0.008)	1.006 (0.009)	1.007 (0.013)	0.993 (0.012)	1.014 (0.011)	JPT (Japanese)	
Mbuti	0.884 (0.024)	1.002 (0.026)	1.03 (0.016)	1.017 (0.016)	Mbuti (2)				CHS (100)	0.996 (0.002)	1.012 (0.009)	1.009 (0.008)	0.999 (0.009)	1.001 (0.013)	0.988 (0.012)	1.008 (0.011)	CHS (Chinese)	
San	0.9 (0.026)	1.009 (0.026)	1.014 (0.016)	1.004 (0.016)	0.99 (0.017)	San (2)				CHB (97)	1.015 (0.01)	1.012 (0.008)	1.002 (0.009)	1.004 (0.013)	0.99 (0.012)	1.011 (0.011)	CHB (Chinese)	
Yoruba	0.863 (0.023)	0.974 (0.025)	0.99 (0.018)	0.982 (0.016)	0.965 (0.016)	0.975 (0.017)	Yoruba (2)				PUR (55)	0.996 (0.005)	0.987 (0.003)	0.992 (0.011)	0.978 (0.01)	0.998 (0.008)	PUR (Pu.Ric.)	
Dai	0.887 (0.027)	1.01 (0.031)	1.012 (0.019)	1.001 (0.021)	0.983 (0.018)	0.999 (0.019)	1.024 (0.019)	Dai (2)				MXL (64)	0.99 (0.004)	0.995 (0.011)	0.981 (0.011)	1.001 (0.009)	MXL (Mexican)	
French	0.874 (0.027)	0.988 (0.031)	0.992 (0.019)	0.978 (0.02)	0.961 (0.019)	0.973 (0.019)	0.997 (0.019)	0.972 (0.018)	French (2)				CLM (60)	1.002 (0.011)	0.989 (0.01)	1.01 (0.008)	CLM (Colomb.)	
Han	0.894 (0.028)	1.014 (0.031)	1.027 (0.018)	1.016 (0.021)	1 (0.019)	1.018 (0.019)	1.044 (0.02)	1.021 (0.017)	1.051 (0.019)	Han (2)				YRI (88)	0.986 (0.004)	1.007 (0.004)	YRI (Nigerian)	
Karitiana	0.862 (0.026)	0.971 (0.028)	0.97 (0.018)	0.961 (0.019)	0.943 (0.018)	0.954 (0.018)	0.975 (0.019)	0.941 (0.019)	0.97 (0.019)	0.923 (0.018)	Karitiana (2)				LWK (96)	1.27 (0.011)	LWK (Kenyan)	
Papuan	0.888 (0.026)	1.011 (0.03)	1.012 (0.021)	0.999 (0.019)	0.982 (0.02)	0.997 (0.018)	1.021 (0.02)	1.002 (0.02)	1.022 (0.018)	0.976 (0.02)	1.057 (0.021)	Papuan (2)				ASW (61)		
Sardinian	0.894 (0.027)	0.989 (0.028)	0.997 (0.018)	0.985 (0.019)	0.967 (0.018)	0.977 (0.018)	1.006 (0.018)	0.978 (0.017)	1.004 (0.017)	0.958 (0.017)	1.035 (0.022)	0.987 (0.018)	Sardinian (2)					
Deep genomes	Denis- ova	Neand- erthal	Dinka	Mand- enka	Mbuti	San	Yoruba	Dai	French	Han	Karitiana	Papuan						

Notes: ±1 standard errors (parentheses) are based on a Block Jackknife with 100 equally sized blocks. Highlighted numbers indicate P < 0.001.

* *R*-ratios computed using Denisova and Neanderthal are normalized by the number of synonymous sites on each lineage, to adjust for the fewer mutations in the ancient sample than on present-day human lineages since divergence (the *R*’ statistic described in the main text). Ratios are based on the accumulation of mutations observed in the population in the row divided by the accumulation of mutations observed in the population shown in the column. The number in parentheses indicates the number of samples per population.

Table S3D – PolyPhen2 “Possibly damaging” mutations for all pairs of 24 deep genomes (bottom left) and 1000 Genomes populations (top right)

			IBS (Spanish)	GBR (British)	FIN (Finnish)	CEU European	JPT Japanese	CHS Chinese	CHB Chinese	PUR Pu.Ric.	MXL Mexican	CLM Colom.	YRI Nigerian	LWK Kenyan	ASW Afr. Am.	1KG	
TSI (98)			1.056 (0.013)	1.024 (0.008)	1.009 (0.012)	1.013 (0.008)	0.969 (0.025)	0.985 (0.027)	0.985 (0.026)	1.045 (0.012)	1.015 (0.018)	1.006 (0.012)	1.057 (0.031)	1.026 (0.028)	1.047 (0.024)	TSI (Italian)	
			IBS (14)	0.969 (0.012)	0.955 (0.013)	0.959 (0.012)	0.921 (0.025)	0.936 (0.026)	0.935 (0.025)	0.991 (0.013)	0.963 (0.018)	0.954 (0.013)	1.014 (0.031)	0.984 (0.028)	1.002 (0.025)	IBS (Spanish)	
	Denisova (1)			GBR (89)	0.985 (0.009)	0.989 (0.006)	0.948 (0.025)	0.963 (0.026)	0.963 (0.025)	1.021 (0.011)	0.992 (0.018)	0.983 (0.011)	1.038 (0.031)	1.007 (0.028)	1.027 (0.024)	GBR (British)	
Neanderthal	0.830 (0.062)	Neanderthal(1)				FIN (93)	1.005 (0.01)	0.961 (0.024)	0.977 (0.026)	0.977 (0.025)	1.036 (0.012)	1.007 (0.018)	0.998 (0.012)	1.05 (0.031)	1.019 (0.028)	1.04 (0.025)	FIN (Finnish)
Dinka	0.808 (0.05)	0.946 (0.065)	Dinka (2)				CEU (85)	0.958 (0.026)	0.973 (0.028)	0.973 (0.027)	1.031 (0.012)	1.002 (0.018)	0.993 (0.012)	1.046 (0.031)	1.015 (0.028)	1.036 (0.024)	CEU (European)
Mandenka	0.842 (0.048)	0.995 (0.06)	1.075 (0.047)	Mandenka (2)				JPT (89)	1.019 (0.01)	1.018 (0.009)	1.075 (0.025)	1.048 (0.023)	1.037 (0.022)	1.084 (0.033)	1.052 (0.03)	1.075 (0.029)	JPT (Japanese)
Mbuti	0.848 (0.048)	0.994 (0.062)	1.043 (0.05)	0.983 (0.044)	Mbuti (2)				CHS (100)	0.999 (0.007)	1.058 (0.025)	1.03 (0.024)	1.02 (0.022)	1.069 (0.033)	1.038 (0.03)	1.06 (0.029)	CHS (Chinese)
San	0.865 (0.047)	1.021 (0.055)	1.043 (0.044)	0.982 (0.038)	1.005 (0.042)	San (2)				CHB (97)	1.058 (0.025)	1.031 (0.023)	1.021 (0.022)	1.07 (0.033)	1.038 (0.031)	1.06 (0.029)	CHB (Chinese)
Yoruba	0.844 (0.044)	0.988 (0.054)	1.017 (0.039)	0.954 (0.036)	0.979 (0.041)	0.966 (0.035)	Yoruba (2)				PUR (55)	0.972 (0.014)	0.964 (0.009)	1.021 (0.026)	0.99 (0.024)	1.009 (0.019)	PUR (Pu.Ric.)
Dai	0.867 (0.057)	1.048 (0.074)	1.075 (0.048)	1.022 (0.047)	1.028 (0.052)	1.049 (0.051)	1.059 (0.048)	Dai (2)				MXL (64)	0.991 (0.011)	1.044 (0.029)	1.014 (0.027)	1.034 (0.023)	MXL (Mexican)
French	0.82 (0.053)	0.988 (0.065)	1.013 (0.048)	0.954 (0.044)	0.968 (0.045)	0.966 (0.044)	0.994 (0.048)	0.931 (0.042)	French (2)				CLM (60)	1.052 (0.028)	1.021 (0.025)	1.041 (0.022)	CLM (Colomb.)
Han	0.881 (0.057)	1.069 (0.072)	1.126 (0.049)	1.055 (0.049)	1.071 (0.05)	1.078 (0.049)	1.102 (0.051)	1.061 (0.048)	1.124 (0.051)	Han (2)				YRI (88)	0.97 (0.008)	0.988 (0.01)	YRI (Nigerian)
Karitiana	0.848 (0.054)	1.031 (0.069)	1.068 (0.052)	1.013 (0.048)	1.008 (0.051)	1.022 (0.049)	1.034 (0.048)	0.976 (0.048)	1.04 (0.053)	0.925 (0.051)	Karitiana (2)				LWK (96)	1.018 (0.011)	LWK (Kenyan)
Papuan	0.868 (0.053)	1.058 (0.07)	1.071 (0.05)	1.008 (0.046)	1.019 (0.047)	1.037 (0.05)	1.05 (0.05)	0.998 (0.049)	1.068 (0.049)	0.952 (0.045)	1.012 (0.054)	Papuan (2)				ASW (61)	
Sardinian	0.851 (0.054)	1.004 (0.061)	1.031 (0.051)	0.968 (0.042)	0.965 (0.043)	0.975 (0.043)	1.013 (0.046)	0.937 (0.042)	1.003 (0.037)	0.881 (0.041)	0.961 (0.05)	0.946 (0.043)	Sardinian (2)				
Deep genomes	Denis-ova	Neanderthal	Dinka	Mandenka	Mbuti	San	Yoruba	Dai	French	Han	Karitiana	Papuan					

Notes: ± 1 standard errors (parentheses) are based on a Block Jackknife with 100 equally sized blocks. Highlighted numbers indicate $P < 0.001$.

* R -ratios computed using Denisova and Neanderthal are normalized by the number of synonymous sites on each lineage, to adjust for the fewer mutations in the ancient sample than on present-day human lineages since divergence (the R' statistic described in the main text). Ratios are based on the accumulation of mutations observed in the population in the row divided by the accumulation of mutations observed in the population shown in the column. The number in parentheses indicates the number of samples per population.

Table S3E – PolyPhen2 “Probably damaging” mutations for all pairs of 24 deep genomes (bottom left) and 1000 Genomes populations (top right)

			IBS (Spanish)	GBR (British)	FIN (Finnish)	CEU European	JPT Japanese	CHS Chinese	CHB Chinese	PUR Pu.Ric.	MXL Mexican	CLM Colomb.	YRI Nigerian	LWK Kenyan	ASW Afr. Am.	1KG
			TSI (98)	IBS (14)												TSI (Italian)
				GBR (89)												IBS (Spanish)
	Denis- ova (1)				FIN (93)											GBR (British)
Neander- thal	0.695 (0.046)	Neand- ertal(1)				CEU (85)										FIN (Finnish)
Dinka	0.724 (0.037)	0.979 (0.058)	Dinka (2)				JPT (89)									CEU (European)
Mandenka	0.734 (0.036)	1.004 (0.055)	1.029 (0.042)	Mand- enka (2)				CHS (100)								JPT (Japanese)
Mbuti	0.734 (0.034)	1.014 (0.048)	1.041 (0.041)	1.026 (0.04)	Mbuti (2)				CHB (97)							CHS (Chinese)
San	0.759 (0.038)	1.026 (0.056)	1.024 (0.039)	1.005 (0.04)	0.98 (0.038)	San (2)										CHB (Chinese)
Yoruba	0.738 (0.036)	1.004 (0.057)	1.007 (0.035)	0.985 (0.039)	0.961 (0.036)	0.975 (0.036)	Yoruba (2)			PUR (55)						PUR (Pu.Ric.)
Dai	0.765 (0.038)	1.066 (0.063)	1.075 (0.046)	1.047 (0.046)	1.013 (0.044)	1.051 (0.04)	1.085 (0.041)	Dai (2)			MXL (64)					MXL (Mexican)
French	0.732 (0.037)	0.993 (0.06)	0.994 (0.045)	0.959 (0.044)	0.937 (0.044)	0.957 (0.04)	0.972 (0.039)	0.908 (0.039)	French (2)			CLM (60)				CLM (Colomb.)
Han	0.762 (0.036)	1.078 (0.057)	1.061 (0.047)	1.048 (0.048)	1.013 (0.039)	1.043 (0.041)	1.08 (0.043)	0.984 (0.041)	1.11 (0.053)	Han (2)			YRI (88)			YRI (Nigerian)
Karitiana	0.712 (0.041)	0.988 (0.062)	0.967 (0.047)	0.938 (0.047)	0.929 (0.045)	0.938 (0.044)	0.96 (0.044)	0.861 (0.041)	0.966 (0.046)	0.875 (0.046)	Karit- iana (2)			LWK (96)	1.027 (0.011)	LWK (Kenyan)
Papuan	0.726 (0.038)	1.008 (0.063)	1.006 (0.052)	0.974 (0.046)	0.964 (0.044)	0.979 (0.044)	0.995 (0.048)	0.924 (0.041)	1.02 (0.048)	0.911 (0.042)	1.046 (0.053)	Papuan (2)			ASW (61)	
Sardinian	0.75 (0.039)	1.001 (0.057)	1.02 (0.046)	0.969 (0.043)	0.958 (0.038)	0.969 (0.043)	0.988 (0.044)	0.919 (0.041)	1.014 (0.045)	0.917 (0.04)	1.052 (0.055)	1.008 (0.048)	Sardinian (2)			
Deep genomes	Denisova	Neander- thal	Dinka	Mand- enka	Mbuti	San	Yoruba	Dai	French	Han	Karit- iana	Papuan				

Notes: ± 1 standard errors (parentheses) are based on a Block Jackknife with 100 equally sized blocks. Highlighted numbers indicate $P < 0.001$.

* R -ratios computed using Denisova and Neanderthal are normalized by the number of synonymous sites on each lineage, to adjust for the fewer mutations in the ancient sample than on present-day human lineages since divergence (the R^* statistic described in the main text). Ratios are based on the accumulation of mutations observed in the population in the row divided by the accumulation of mutations observed in the population shown in the column. The number in parentheses indicates the number of samples per population.

Table S4: Expected $R_{WestAfrica/Europe}$ for different models of demography

	$R^{All\ non-synonymous}$	R^{Benign}	$R^{Possibly\ damaging}_A$	$R^{Probably\ damaging}$
Estimated percentage of sites in each of three selective coefficient bins				
Percent of sites that are neutral	19%	27%	16%	9%
Percent of sites with weak selection coefficients: $s = -10^{-3}$	47%	60%	54%	27%
Percent of sites with strong selection coefficients: $s = -10^{-2}$	33%	13%	29%	64%
Model of history simulated				
Tennessen⁴	0.989	0.990	0.985	0.988
Gravel⁵	0.987	0.988	0.984	0.986
Lohmueller²	0.992	0.993	0.989	0.991

Notes: As described in Note S1, we assume that selective coefficients take on only one of three values: $s = 0$ (“neutral”), -10^{-3} (“weak”), and -10^{-2} (“strong”), and then fit the density in each of these bins using site frequency spectrum data under the assumption of mutations all acting additively with no epistasis. In the bottom section of the table, we show the value of $R_{WestAfrica/Europe}$ expected for each demographic model and distribution of selective coefficients. The expected values are less than two standard errors from 1 (using the Block Jackknife standard errors from Table 1), indicating that do not expect much difference in the accumulation of deleterious mutations in Europeans than in West Africans.

Table S5: $R_{\text{African/Non-African}}$ -statistic stratified by time depth of comparison

	$R(\text{synonymous})$	$R(\text{All non-synonymous})$	$R(\text{Benign})$	$R(\text{Possibly damaging})$	$R(\text{Probably damaging})$
[0.0008-ancient)	1.046 (0.014)	1.050 (0.017)	1.063 (0.019)	0.976 (0.059)	1.025 (0.053)
[0.0004-0.0008)	1.018 (0.022)	1.026 (0.028)	1.005 (0.046)	1.028 (0.101)	1.012 (0.057)
[0-0.0004)	1.008 (0.033)	1.009 (0.044)	0.931 (0.061)	1.017 (0.145)	1.146 (0.093)

Notes: ± 1 standard errors are from a Block Jackknife with 20 equally sized contiguous blocks. For this analysis, we compare 4 sub-Saharan African to 6 non-African phased genomes. We restrict to sites that have a GATK genotype quality of ≥ 70 , and that furthermore have a consistent genotype between GATK and samtools. The time stratification is in units of heterozygosity expected for segments of this time depth.

Table S6A: Unnormalized R_{XY} statistics: bottom left GC→AT, top right AT→GC

Notes: Ratios are based on the accumulation of mutations observed in the population in the row divided by the accumulation of mutations observed in the population in the column. The number in parentheses indicates the number of samples per population. \pm standard errors (parentheses) are based on a Block Jackknife. Highlighted numbers indicate $P < 0.001$. We observe significant deviations from one in most pairwise comparisons. This could be due to different error rates across samples which are small but significant given the small standard errors, or different mutation rates across samples. We therefore correct for such systematic differences across samples in Table S6B by normalizing by the substitution rate differences at G/C and A/T sites, which are not subject to biased gene conversion.

Table S6B: Normalized R'_{XY} statistics: bottom left GC→AT, top right AT→GC

			Genetic Distances														
			Papuan	Karit-iana	Han	French	Dai	Yoruba	San	Mbuti	Mand-enka	Dinka	Denisova	Neander-thal			
	Sardinian (2)	1.001 (0.003)	1.002 (0.003)	0.996 (0.003)	0.994 (0.003)	0.998 (0.003)	0.994 (0.003)	0.998 (0.002)	0.996 (0.002)	0.999 (0.003)	0.997 (0.002)	1.058 (0.003)	1.009 (0.003)	Sardinian			
	Papuan (2)	1.001 (0.003)	0.995 (0.003)	0.994 (0.003)	0.996 (0.003)	0.994 (0.003)	0.997 (0.003)	0.996 (0.003)	0.998 (0.003)	0.996 (0.003)	1.059 (0.004)	1.008 (0.003)	Papuan				
			Karit-iana (2)	0.993 (0.003)	0.992 (0.003)	0.994 (0.003)	0.993 (0.003)	0.996 (0.003)	0.994 (0.003)	0.998 (0.003)	0.995 (0.002)	1.057 (0.004)	1.008 (0.003)	Karitiana			
Denisova	1.041 (0.005)	Denisova (1)			Han (2)	0.999 (0.003)	1.001 (0.003)	0.998 (0.003)	1.001 (0.003)	1 (0.003)	1.002 (0.003)	1 (0.002)	1.059 (0.004)	1.011 (0.003)	Han		
Dinka	0.965 (0.003)	0.928 (0.004)	Dinka (2)				French (2)	1.003 (0.003)	0.999 (0.003)	1.002 (0.002)	1 (0.002)	1.004 (0.002)	1.001 (0.002)	1.06 (0.003)	1.01 (0.003)	French	
Mand-enka	0.963 (0.003)	0.927 (0.004)	0.998 (0.002)	Mand-enka (2)				Dai (2)	0.997 (0.003)	1.001 (0.003)	0.998 (0.002)	1.001 (0.003)	0.999 (0.002)	1.059 (0.004)	1.009 (0.003)	Dai	
Mbuti	0.964 (0.003)	0.927 (0.004)	0.997 (0.002)	1 (0.003)	Mbuti (2)				Yoruba (2)	1.003 (0.003)	1.002 (0.002)	1.005 (0.002)	1.004 (0.002)	1.063 (0.003)	1.013 (0.003)	Yoruba	
San	0.956 (0.003)	0.92 (0.004)	0.987 (0.002)	0.99 (0.002)	0.989 (0.003)	San (2)				San (2)	0.999 (0.002)	1.002 (0.003)	1 (0.002)	1.061 (0.003)	1.013 (0.003)	San	
Yoruba	0.961 (0.003)	0.925 (0.004)	0.995 (0.002)	0.998 (0.002)	0.997 (0.002)	1.009 (0.002)	Yoruba (2)				Mbuti (2)	1.003 (0.002)	1.001 (0.002)	1.063 (0.003)	1.013 (0.003)	Mbuti	
Dai	0.958 (0.003)	0.925 (0.004)	0.995 (0.002)	0.998 (0.003)	0.997 (0.003)	1.009 (0.002)	1.000 (0.002)	Dai (2)				Mand-enka (2)	0.998 (0.002)	1.06 (0.003)	1.01 (0.003)	Mandenka	
French	0.963 (0.003)	0.929 (0.004)	1.002 (0.002)	1.005 (0.002)	1.004 (0.003)	1.015 (0.002)	1.007 (0.002)	1.009 (0.003)	French (2)					Dinka (2)	1.06 (0.003)	1.012 (0.003)	Dinka
Han	0.961 (0.003)	0.927 (0.004)	0.997 (0.002)	1 (0.002)	1 (0.003)	1.01 (0.002)	1.003 (0.003)	1.003 (0.002)	0.995 (0.003)	Han (2)				Denisova (1)	0.945 (0.004)	Denisova	
Karitiana	0.959 (0.003)	0.924 (0.004)	0.993 (0.003)	0.997 (0.003)	0.996 (0.003)	1.007 (0.003)	0.999 (0.003)	0.998 (0.003)	0.99 (0.003)	0.995 (0.003)	Karitiana (2)				Neander-thal (1)		
Papuan	0.959 (0.003)	0.924 (0.004)	0.995 (0.002)	0.997 (0.003)	0.997 (0.003)	1.008 (0.003)	1.000 (0.003)	0.999 (0.002)	0.992 (0.003)	0.997 (0.003)	1.001 (0.003)	Papuan (2)					
Sardinian	0.963 (0.003)	0.929 (0.004)	1.001 (0.002)	1.003 (0.002)	1.003 (0.002)	1.014 (0.002)	1.006 (0.002)	1.007 (0.003)	0.998 (0.003)	1.004 (0.003)	1.008 (0.003)	0.997 (0.003)	Sardinian (2)				
	Neander-thal	Denisova	Dinka	Mand-enka	Mbuti	San	Yoruba	Dai	French	Han	Karitiana	Papuan					

Notes: Ratios are based on the accumulation of mutations observed in the population in the row divided by the accumulation of mutations observed in the population in the column. The number in parentheses indicates the number of samples per population. ± 1 standard errors (parentheses) are based on a Weighted Block Jackknife.

Highlighted numbers indicate $P < 0.001$. Ratios are normalized by the sum of $A \rightarrow T$, $T \rightarrow A$, $C \rightarrow G$ and $G \rightarrow C$ mutations on each lineage, producing an R^* statistic that adjusts for differences in the rates of accumulations of mutations on different lineages since divergence. These differences can arise due to branch shortening in the archaic lineages, or to different rates of mutation in the different populations. By normalizing, we highlight any differences in rates that are above and beyond these processes.

Table S7: Key statistics as a function of allelic substitution patterns

Substitution type	Benign	Possibly damaging	Probably damaging	Non- synonymous
<i>R_{WestAfrica/Europe}</i>				
C→T or G→A	0.981 (0.028)	0.942 (0.059)	0.978 (0.053)	0.976 (0.023)
T→C or A→G	1.035 (0.034)	0.995 (0.082)	0.941 (0.102)	1.023 (0.029)
A→C or T→G	1.016 (0.054)	1.127 (0.112)	1.183 (0.089)	1.082 (0.042)
C→A or G→T	1.001 (0.060)	1.213 (0.127)	1.113 (0.114)	1.065 (0.051)
A→T or T→A	1.017 (0.100)	0.995 (0.188)	0.927 (0.136)	1.001 (0.076)
C→G or G→C	0.971 (0.049)	0.957 (0.082)	1.078 (0.093)	0.989 (0.038)
All but C→T or G→A	1.018 (0.021)	1.053 (0.051)	1.073 (0.052)	1.033 (0.017)
All sites	1.002 (0.018)	1.007 (0.040)	1.031 (0.038)	1.008 (0.015)
<i>R'_{WestAfrica/Europe}</i>				
C→T or G→A	0.956 (0.030)	0.918 (0.058)	0.953 (0.049)	0.951 (0.025)
T→C or A→G	1.005 (0.043)	0.966 (0.084)	0.914 (0.099)	0.993 (0.038)
A→C or T→G	1.009 (0.080)	1.118 (0.134)	1.173 (0.134)	1.074 (0.084)
C→A or G→T	1.055 (0.087)	1.278 (0.146)	1.172 (0.145)	1.122 (0.084)
A→T or T→A	1.060 (0.143)	1.039 (0.209)	0.968 (0.158)	1.044 (0.117)
C→G or G→C	0.945 (0.064)	0.931 (0.096)	1.049 (0.106)	0.962 (0.060)
All but C→T or G→A	1.004 (0.029)	1.038 (0.052)	1.059 (0.051)	1.019 (0.024)
All sites	0.981 (0.022)	0.986 (0.041)	1.010 (0.037)	0.987 (0.019)
<i>R'_{AllModern/Denisova}</i>				
C→T or G→A	0.898 (0.035)	0.828 (0.065)	0.565 (0.033)	0.812 (0.027)
T→C or A→G	0.860 (0.046)	0.904 (0.120)	0.697 (0.091)	0.851 (0.042)
A→C or T→G	0.830 (0.119)	0.725 (0.143)	1.475 (0.313)	0.908 (0.117)
C→A or G→T	1.085 (0.127)	0.789 (0.123)	1.080 (0.189)	1.026 (0.103)
A→T or T→A	0.848 (0.162)	0.919 (0.228)	0.791 (0.227)	0.857 (0.149)
C→G or G→C	0.766 (0.075)	0.799 (0.118)	1.244 (0.207)	0.833 (0.072)
All but C→T or G→A	0.865 (0.039)	0.810 (0.058)	0.985 (0.070)	0.872 (0.034)
All sites	0.929 (0.029)	0.870 (0.046)	0.760 (0.035)	0.889 (0.024)
<i>R'_{AllModern/Neanderthal}</i>				
C→T or G→A	0.953 (0.040)	0.994 (0.094)	0.909 (0.059)	0.953 (0.033)
T→C or A→G	1.046 (0.056)	1.053 (0.126)	0.928 (0.156)	1.038 (0.051)
A→C or T→G	0.937 (0.105)	1.132 (0.197)	1.462 (0.283)	1.085 (0.105)
C→A or G→T	1.073 (0.125)	0.991 (0.160)	1.188 (0.201)	1.086 (0.112)
A→T or T→A	0.988 (0.214)	0.786 (0.208)	0.928 (0.224)	0.944 (0.168)
C→G or G→C	0.816 (0.070)	1.099 (0.173)	1.169 (0.185)	0.919 (0.077)
All but C→T or G→A	0.997 (0.037)	1.074 (0.079)	1.181 (0.092)	1.037 (0.036)
All sites	0.993 (0.026)	1.065 (0.062)	1.063 (0.054)	1.015 (0.025)
<i>R'_{Denisova/Neanderthal}</i>				
C→T or G→A	1.089 (0.060)	1.210 (0.147)	1.695 (0.160)	1.215 (0.055)
T→C or A→G	1.250 (0.098)	1.072 (0.182)	1.409 (0.277)	1.244 (0.087)
A→C or T→G	1.049 (0.184)	1.594 (0.447)	0.687 (0.201)	1.083 (0.170)
C→A or G→T	0.849 (0.128)	1.188 (0.266)	1.133 (0.251)	0.966 (0.136)
A→T or T→A	1.195 (0.275)	0.913 (0.272)	1.141 (0.387)	1.135 (0.218)
C→G or G→C	1.027 (0.138)	1.368 (0.323)	1.029 (0.204)	1.091 (0.126)
All but C→T or G→A	1.132 (0.068)	1.290 (0.118)	1.172 (0.140)	1.164 (0.059)
All sites	1.064 (0.044)	1.198 (0.090)	1.433 (0.096)	1.141 (0.040)

Notes: ± 1 standard errors are from a Block Jackknife. Statistics computed using Denisova and Neanderthal are normalized by the number of synonymous sites on each lineage, to adjust for the fact that there has been less time for mutations to accumulate in the ancient lineages than present-day human lineages since divergence (the R' statistic in the main text). Red highlighting indicates a nominal $P < 0.001$ for $R < 1$ or $R' < 1$, and green highlighting indicates a nominal $P < 0.001$ for $R > 1$ or $R' > 1$. These results document a significantly higher burden of deleterious mutations in Denisova than in present-day humans whether the analysis is performed over all sites or excluding C→T and G→A sites which are known to be subject to high rates of error in ancient DNA. There is no clear evidence of a higher load of deleterious mutations in Neanderthals compared with present-day humans.

Table S8: R^2 -statistic for all population pairs

	Dinka (2)										
Mand-enka	0.927 (0.038)	Mand-enka (2)									
Mbuti	0.956 (0.036)	1.025 (0.038)	Mbuti (2)								
San	0.907 (0.032)	0.962 (0.036)	0.949 (0.036)	San (2)							
Yoruba	0.92 (0.041)	0.99 (0.04)	0.969 (0.035)	1.029 (0.038)	Yoruba (2)						
Dai	1.601 (0.066)	1.684 (0.064)	1.609 (0.065)	1.681 (0.065)	1.713 (0.071)	Dai (2)					
French	1.448 (0.06)	1.528 (0.066)	1.454 (0.06)	1.513 (0.064)	1.541 (0.066)	0.879 (0.034)	French (2)				
Han	1.608 (0.059)	1.677 (0.07)	1.605 (0.064)	1.691 (0.068)	1.702 (0.072)	1.009 (0.036)	1.142 (0.045)	Han (2)			
Karitiana	2.141 (0.078)	2.228 (0.082)	2.091 (0.077)	2.147 (0.079)	2.239 (0.085)	1.468 (0.054)	1.619 (0.06)	1.455 (0.052)	Karitiana (2)		
Papuan	1.879 (0.07)	1.963 (0.078)	1.867 (0.058)	1.925 (0.064)	1.975 (0.067)	1.214 (0.048)	1.358 (0.048)	1.203 (0.049)	0.866 (0.032)	Papuan (2)	
Sardinian	1.524 (0.057)	1.603 (0.063)	1.522 (0.059)	1.579 (0.059)	1.612 (0.058)	0.936 (0.034)	1.064 (0.038)	0.933 (0.034)	0.655 (0.025)	0.787 (0.029)	Sardinian (2)
	Dinka	Mand-enka	Mbuti	San	Yoruba	Dai	French	Han	Karitiana	Papuan	

Notes: ± 1 standard errors (parentheses) are based on a Block Jackknife. Highlighted numbers indicate $P < 0.001$.

* For all population pairs, we show the R^2_{XY} statistic. Ratios are based on the expected rate in the population in the row divided by the expected rate in the population in the column. Number in parentheses indicates the samples per population.

Table S9: Parameters of simulated demographic models

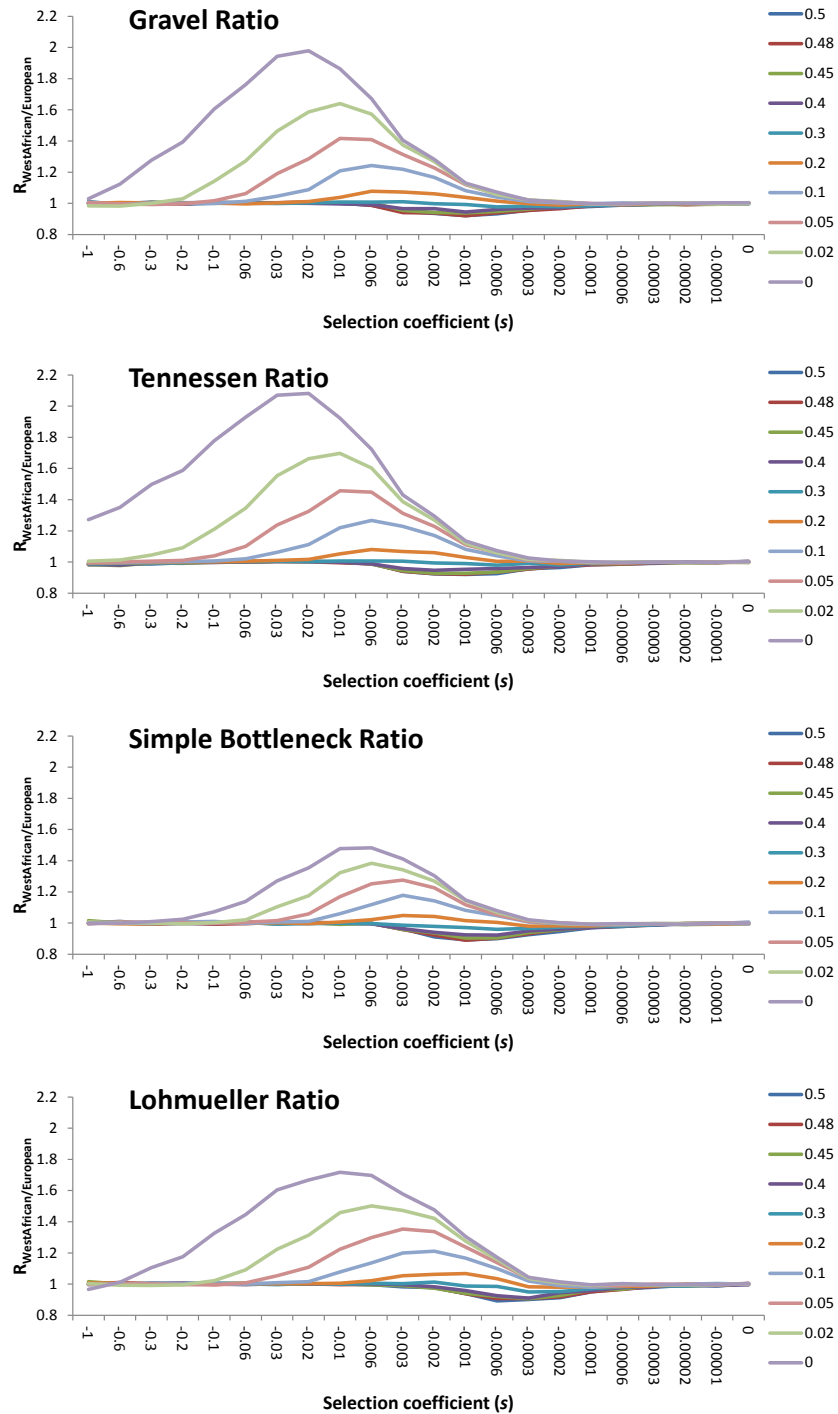
Gravel⁵ [$\pi_{Eur}/\pi_{Afr}=0.72$; $F_{ST}(Eur,Afr)=0.19$]			Simple bottleneck [$\pi_{Eur}/\pi_{Afr}=0.69$; $F_{ST}(Eur,Afr)=0.21$]		
<i>Time in gens.</i>	$2N_{Afr}$	$2N_{Eur}$	<i>Time in gens.</i>	$2N_{Afr}$	$2N_{Eur}$
$300000 \leq t < 3880$	28948		$300000 \leq t < 3880$	28948	
$3880 \leq t < 5000$	28948	3,722	$3880 \leq t < 4080$	28948	500
$5000 \leq t \leq 5921$	28948	$2064e^{.003858(t-5000)}$	$4080 \leq t \leq 5921$	28948	28948

Tennessen⁴ [$\pi_{Eur}/\pi_{Afr}=0.70$; $F_{ST}(Eur,Afr)=0.21$]			Lohmueller² [$\pi_{Eur}/\pi_{Afr}=0.70$; $F_{ST}(Eur,Afr)=0.29$]		
<i>Time in gens.</i>	$2N_{Afr}$	$2N_{Eur}$	<i>Time in gens.</i>	$2N_{Afr}$	$2N_{Eur}$
$300000 \leq t < 3880$	28948		$300000 \leq t < 100002$	15672	
$3880 \leq t < 5000$	28,948	3,722	$100002 \leq t < 101772$	15556	11398
$5000 \leq t < 5716$	28,948	$2064e^{.00307(t-5000)}$	$101772 \leq t < 107706$	51272	11398
$5716 \leq t \leq 5921$	$28948e^{.00166(t-5716)}$	$18900e^{.00195(t-5716)}$	$107706 \leq t \leq 108580$	51272	60060

Notes: All simulations use $\mu = 2 \times 10^{-8}$ and burn in from generation 250,000 to 0. The switch from sampling every 100 to every 1 generations occurs at 1000 for the three models that end at time 5,921, and at +99,000 for the Lohmueller model². Summary statistics at the end of the simulation are shown; F_{ST} is computed based on all SNPs, resulting in a higher differentiation than calculations that restrict to common SNPs.

Figure S1 – $R_{WestAfrica/Europe}$ for four demographic histories (simulations)

We show the expected accumulation of deleterious mutation in West Africans compared with Europeans at the present. We explore a range of selection coefficients s and dominance coefficients h , for the four models of demographic history specified in Table S9. The left column gives the ratio and the right column the difference. We observe a greater accumulation of deleterious mutations in West Africans for recessively acting mutations ($h=0$), and a greater accumulation in Europeans for additively acting mutations ($h=0.5$).



Supplementary References

1. Meyer, M. *et al.* A high-coverage genome sequence from an archaic Denisovan individual. *Science* **338**, 222-6 (2012).
2. Lohmueller, K.E. *et al.* Proportionally more deleterious genetic variation in European than in African populations. *Nature* **451**, 994-7 (2008).
3. Abecasis, G.R. *et al.* An integrated map of genetic variation from 1,092 human genomes. *Nature* **491**, 56-65 (2012).
4. Tennessen, J.A. *et al.* Evolution and functional impact of rare coding variation from deep sequencing of human exomes. *Science* **337**, 64-9 (2012).
5. Gravel, S. *et al.* Demographic history and rare allele sharing among human populations. *Proc Natl Acad Sci U S A* **108**, 11983-8 (2011).

Note S1: Inferred distributions of selection coefficients for PolyPhen-2 classes

Abstract

This note details the empirical fitting of the site frequency spectrum (SFS) from 1000 genomes data to determine the underlying distribution of fitness effects (DFE) for new mutations. Of particular interest is the DFE for PolyPhen2 classes.

Aims and goals

Here we describe the technique used to analyze the distribution of selective effects of de novo mutations that form the distribution of fitness effects (DFE). Our primary aim is to infer this distribution from the site frequency spectrum of polymorphic non-synonymous alleles in the context of a given demographic history and total mutation rate. The de novo DFE in humans is in principle independent of population history and other demographic differences between individuals, allowing us to infer the distribution from a single fixed demography without loss of generality, provided the demographic inference is accurate.

1 Site frequency spectra

We use coding sequences from the 1000 genomes Yoruban (YRI) and Northern Europeans from Utah (CEU) populations to create a site frequency spectrum (SFS) in the form of a minor allele frequency (MAF) spectrum for both synonymous and non-synonymous sites. Additionally, we stratify the non-synonymous SFS by predicted PolyPhen2 classes, labeled benign, possibly damaging, and probably damaging in order of increased predicted effect.

1.1 Simulated MAFs

Using the demographic inferences given in Gravel, et al.[4], we simulate a genome of length 100Mb through the inferred demographic histories of European and African populations for a range of selective effects. In particular, the simulator tracks the derived allele frequencies of 10^8 independently evolving sites, in the infinite recombination limit with no linkage.

Mutations are introduced at a rate $\mu = 2 \times 10^{-8}$ per site per individual per generation. The population size is time dependent and reflects the demography associated with the population of interest. After completing roughly 5000 generations of recent demographic history, the allele frequencies are subsampled to the sample size of the associated 1000 genomes population sample, 88 for YRI and 85 for CEU. The results of this simulation provide expectations for the MAF for alleles with a single selective coefficient s . We simulate separately for $s = \{0, -10^{-3}, -10^{-2}\}$, which we consider to be neutral, weakly deleterious, and strongly deleterious, respectively. These selective coefficients are chosen to represent the range of realistic selective effects expected to be segregating in the human population. Alleles of stronger selective effect are likely to be absent in all but the largest population samples, and will be incorporated into the $s = -10^{-2}$ fitness class in our fit. These simulated MAFs provide the basis for our fit, as we will estimate the coefficients of their linear combination to determine the DFE.

2 Overall scale and target size

The number of bases simulated clearly overestimates the length of the human coding genome. The total coding genome is thought to be roughly $30Mb$ long, accounting for about 1% of the whole genome. Since estimates of both the mutation rate and target size are known to be relatively imprecise, we use the synonymous MAF to determine the overall rescaling for fitting our simulations to 1000 genomes data. Additionally, this method accounts for coverage issues, etc., assuming the same fraction of synonymous and non-synonymous sites are affected.

2.1 Scale factor for synonymous sites

Assuming synonymous sites are selectively neutral, we use a maximum likelihood fit with a single parameter to determine the scale factor for synonymous sites. The log likelihood is calculated as follows.

$$\log \mathcal{L} = \sum_{i=1}^N (D_i \log[F_i] - F_i) \quad (1)$$

Here D_i represents the i^{th} bin of the MAF from data, where $i \in [1, N]$ corresponds to allele count in the sample ranging from singletons at frequency $x = i/2N = 1/2N$ to alleles present in half of the haploid individuals at $x = N/2N = 1/2$. Similarly, F_i corresponds to counts in the fit to simulation, and is a function of fit parameters ϵ_k . For the present purposes, we are interested in determining the maximum likelihood for the following form of $F_i(\epsilon)$.

$$F_i(\epsilon) = \epsilon S_0^i \quad (2)$$

S_0^i represents the i^{th} count of the MAF for the appropriately down-sampled neutral simulation with $s = 0$. The maximum log likelihood is given by the following expression.

$$\max[\log \mathcal{L}(\epsilon^{syn})] = \max \left[\sum_{i=1}^N (D_i \log[\epsilon^{syn} S_0^i] - \epsilon^{syn} S_0^i) \right] \quad (3)$$

We use the YRI synonymous MAF $D_i^{YRI_{syn}}$ and the simulated YRI MAF for $s = 0$ to determine $\epsilon^{YRI_{syn}}$ numerically. The synonymous scale factor for YRI is determined by the maximum log likelihood value at $\epsilon^{YRI_{syn}} = 0.093$. Analogously, the synonymous scale factor for CEU has a maximum log likelihood value of $\epsilon^{CEU_{syn}} = 0.097$.

2.2 Scale factor for non-synonymous sites

Kryukov, et al. [1] estimates the synonymous and non-synonymous fractions of the coding genome to be 0.32 and 0.68, respectively. This can be used to determine the appropriate scale factor for non-synonymous sites. The scale factor is simply the ratio of the total mutation rate in the target to the total simulated mutation rate.

$$\epsilon^{syn} = \frac{U_{syn}^{data}}{U_{syn}^{sim}} = \frac{(\mu L_{syn})}{U_{syn}^{sim}} \quad (4)$$

This can be solved for μ and substituted in to the non-synonymous expression to determine the non-synonymous scale factor.

$$\begin{aligned} \epsilon^{nonsyn} &= \frac{U_{nonsyn}^{data}}{U_{nonsyn}^{sim}} = \frac{(\mu L_{nonsyn})}{U_{nonsyn}^{sim}} \\ &= \frac{L_{nonsyn}}{L_{syn}} \epsilon^{syn} = \left(\frac{68}{32} \right) \epsilon^{syn} \end{aligned} \quad (5)$$

We find the following scale factors for the YRI and CEU simulated data.

ϵ_{nonsyn}^{YRI}	ϵ_{nonsyn}^{CEU}
0.198	0.207

2.3 Scale factors for Polyphen2 classes

The Polyphen2 software provides functional predictions that can be stratified into 3 classes: benign, possibly damaging, and probably damaging. One can compute the target size of these classes as a fraction of the total non-synonymous coding genome. This is accomplished by enumerating all possible point mutations from the hg19 human reference genome and classifying each mutation. We use the context dependent 64×4 weight matrix of single point mutations from a given triplet to all others [2]. Each of the 4^3 possible triplets has an associated matrix. Using HumVar, we compute approximate fractions for PolyPhen2 classes found in the following table.

prediction	fraction (%)
benign	50.0
possibly damaging	16.7
probably damaging	33.3
unknown*	$\ll 1$

To confirm that this estimate is not biased by ancestry or recent demography, we stratify the human reference genome by predicted ancestry and find no substantial difference from these approximate values. From these fractions, we compute the appropriate scale factors for our fitting procedure.

ϵ_{benign}^{YRI}	$\epsilon_{possibly}^{YRI}$	$\epsilon_{probably}^{YRI}$
0.099	0.033	0.066

ϵ_{benign}^{CEU}	$\epsilon_{possibly}^{CEU}$	$\epsilon_{probably}^{CEU}$
0.104	0.035	0.069

3 Maximum Likelihood fit

Using the scale factors determined in the previous section, we compute the maximum log likelihood for a linear combination of selective effects. For simplicity, we choose to represent the DFE as a sum of several single s effect classes, rather than using a continuous functional form. We acknowledge that this three point mass model is a simplification of the true distribution of selection coefficients, but believe that it is useful for the purpose of obtaining a rough prediction of the expected value of the R-statistic for specific PolyPhen-2 classes.

$$\log \mathcal{L}(\{\alpha_k\}) = \sum_{i=1}^N (D_i \log[F_i(\{\alpha_k\})] - F_i(\{\alpha_k\})) \quad (6)$$

We use the following form for the fit function $F(\{\alpha_k\})$.

$$F_i(\{\alpha_k\}) = \epsilon^{nonsyn} \sum_k \alpha_k S_k^i = \epsilon^{nonsyn} (\alpha_0 S_0^i + \alpha_3 S_3^i + \alpha_2 S_2^i) \quad (7)$$

We employ the notation $k = 0$ for the simulated $s = 0$ MAF, $k = 3$ for the simulated $s = -10^{-3}$ MAF, and $k = 2$ for the simulated $s = -10^{-2}$ MAF. In this form, S_i^3 represents the MAF for the weakly selected sites, and α_3 is the fraction of the DFE that falls into this category. By estimating the maximum likelihood we can re-assemble the DFE in a rudimentary form as a fraction of mutations that fall into the category of neutral, weakly deleterious, and strongly deleterious. Since the overall scale factor is fixed, the α_k coefficients must be normalized with the following constraint.

$$\sum_k \alpha_k = 1 \quad (8)$$

This restricts the fit function as follows.

$$F_i(\{\alpha_k\}) = \epsilon^{nonsyn} (\alpha_0 S_0^i + \alpha_3 S_3^i + (1 - \alpha_0 - \alpha_3) S_2^i) \quad (9)$$

Note that for the present purposes, we have chosen 2 free parameters to fit, such that $\{\alpha_k\} = \{\alpha_0, \alpha_3\}$. For a 3 parameter fit with an additional nearly neutral class at $s = -10^{-4}$, for example, we simply introduce α_4 and S_4^i and modify the constraint $(\alpha_0 + \alpha_3 + \alpha_4 + \alpha_2) = 1$, with free parameters $\{\alpha_k\} = \{\alpha_0, \alpha_4, \alpha_3\}$. This method can be easily extended to fit an arbitrary number of parameters by including additional S_k^i for various selective effects. We have found this unnecessary for the present purposes, as it results in the effective overfitting of the DFE.

The maximum likelihood fit for 2 parameters is given simply by the following equations.

$$\max [\log \mathcal{L}(\alpha_0, \alpha_3)] = \max \left[\sum_{i=1}^N (D_i \log[F_i(\{\alpha_k\})] - F_i(\{\alpha_k\})) \right] \quad (10)$$

$$F_i(\{\alpha_k\}) = \epsilon^{nonsyn} (\alpha_0 S_0^i + \alpha_3 S_3^i + (1 - \alpha_0 - \alpha_3) S_2^i) \quad (11)$$

4 Results

Using the method outlined above, we compute the maximum likelihood fits for various PolyPhen2 classes using YRI, CEU, and a joint measure that is the sum of the log likelihood functions of both YRI and CEU. Since the DFE should in principle be independent of demographic history, one can use the overlap of the independent measures in YRI and CEU in the form of the joint log likelihood (defined as a sum of the two log likelihoods) to produce a fit that is less sensitive to demographic errors in either of the two populations individually. The maximum log likelihood fit is summarized in the tables below. Errors are given for the joint fit, as this will be used in our subsequent analysis.

2 parameter fit (YRI)	neutral ($s = 0$)	weak ($s = -10^{-3}$)	strong ($s = -10^{-2}$)
all non-synonymous	0.20	0.44	0.36
benign	0.28	0.56	0.16
possibly damaging	0.17	0.50	0.34
probably damaging	0.09	0.25	0.66

2 parameter fit (CEU)	neutral ($s = 0$)	weak ($s = -10^{-3}$)	strong ($s = -10^{-2}$)
all non-synonymous	0.18	0.55	0.27
benign	0.26	0.68	0.06
possibly damaging	0.15	0.63	0.21
probably damaging	0.08	0.32	0.60

2 parameter fit (Joint)	neutral ($s = 0$)	weak ($s = -10^{-3}$)	strong ($s = -10^{-2}$)
all non-synonymous	0.19 ± 0.01	0.47 ± 0.04	0.33 ± 0.05
benign	0.27 ± 0.02	0.60 ± 0.07	0.13 ± 0.07
possibly damaging	0.16 ± 0.03	0.54 ± 0.11	0.29 ± 0.11
probably damaging	0.09 ± 0.01	0.27 ± 0.06	0.64 ± 0.06

4.1 Log Likelihood plots

The log likelihood surface for the two parameter fit can be visualized in a contour plot shown in Figure 1. We note that the normalization condition $\sum_k \alpha_k = 1$ determines the strongly deleterious class uniquely. Figure 2 plots log likelihood contours for the benign, possibly damaging, and probably damaging PolyPhen2 classes. We note a trend in the location of

the maximum towards smaller values with increased predicted effect. All of the mass that vanishes in this process contributes to enhancing the weight of the strongly deleterious class. This is consistent with the stratification by PolyPhen2 score, reinforcing our results.

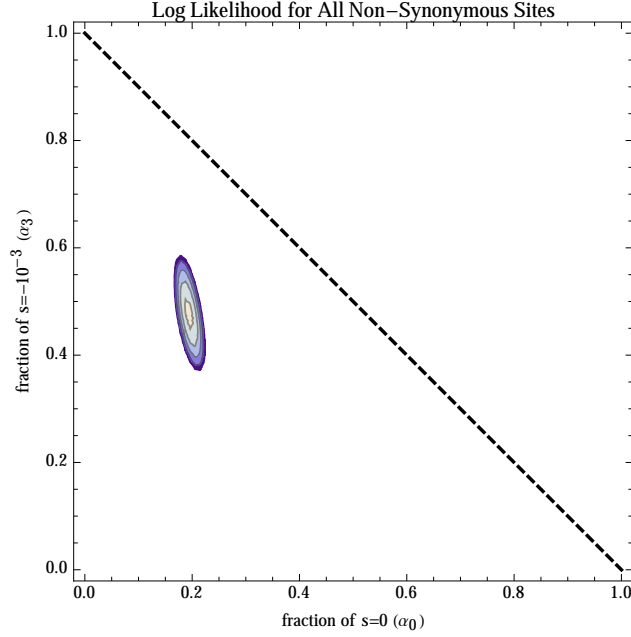


Figure 1: The log likelihood plot for the joint inference from YRI and CEU data for all non-synonymous sites is shown for a two parameter fit. Contours are plotted representing two standard deviations from the peak. The coefficients of $s = 0$ and $s = -10^{-3}$, represented as (α_0, α_3) , are plotted on the x and y axes, respectively. The fraction of strongly deleterious ($s = -10^{-2}$) sites in the DFE is constrained by the equation $\alpha_0 + \alpha_3 + \alpha_2 = 1$. This constraint restricts allowed values to below the dashed line. The maximum likelihood fit is located at $\{\alpha_0, \alpha_3, \alpha_2\} = \{0.19, 0.47, 0.33\}$.

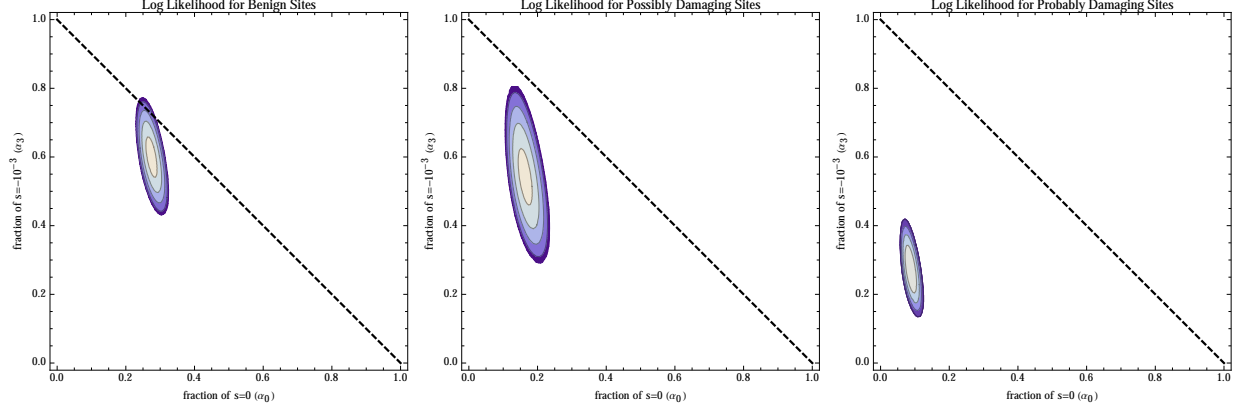


Figure 2: Log Likelihood plots for the 2 parameter fit from the joint inference of YRI and CEU data are plotted for PolyPhen2 classes. **LEFT:** Benign sites. **MIDDLE:** Possibly damaging sites. **RIGHT:** Probably damaging sites. All plots have axes (α_0, α_3) corresponding to neutral and weakly deleterious alleles and display two standard deviations from the maximum. The constraint $\alpha_0 + \alpha_3 + \alpha_2 = 1$ is satisfied, and only values below the dashed line are allowed. Note that the fit favors smaller fractions of neutral and weakly deleterious sites in favor of strongly deleterious sites with increasing PolyPhen2 score, consistent with prediction.

5 Using the DFE to appropriately weight R

Here we use the inferred distribution of fitness effects, $\rho(s)$, to define an expected value $\langle R \rangle$ corresponding to the value of R that we expect to observe in population data. The appropriately weighted mutation load $\langle L \rangle$ for a given population is given by convoluting the load at different s values over the DFE.

$$\langle L \rangle = \int ds \rho(s) L(s) \quad (12)$$

This is true for both populations independently, since the DFE is roughly the same, allowing us to compute the expected $\langle R \rangle$ as follows.

$$\langle R \rangle = \frac{\langle L \rangle_{pop0}}{\langle L \rangle_{pop1}} = \frac{\int ds \rho(s) L^{pop0}(s)}{\int ds \rho(s) L^{pop1}(s)} \quad (13)$$

For the discretization of the DFE into neutral, weakly deleterious, and strongly deleterious components, this can be rewritten as the following sum.

$$\begin{aligned} \langle R \rangle &= \frac{\sum_k \alpha_k L^{pop0}(s_k)}{\sum_k \alpha_k L^{pop1}(s_k)} \\ &= \frac{\alpha_0 L^{pop0}(s=0) + \alpha_3 L^{pop0}(s=-10^{-3}) + \alpha_2 L^{pop0}(s=-10^{-2})}{\alpha_0 L^{pop1}(s=0) + \alpha_3 L^{pop1}(s=-10^{-3}) + \alpha_2 L^{pop1}(s=-10^{-2})} \end{aligned} \quad (14)$$

Here the α_k correspond to the fractions given in the results table above, and can represent appropriate values for all non-synonymous sites, or those for any of the PolyPhen2 classes.

5.1 Computing $\langle R \rangle$, the weighted R statistic

Here, we calculate a weighted mutation load for population 0 (African) and population 1 (European) using fractions obtained from the maximum likelihood fits from the inferred distribution of fitness effects from Section 4 and from simulated mutation loads for average selection coefficients $s = \{0, -0.001, -0.01\}$. We calculated the weighted R statistic, denoted $\langle R \rangle$, as the ratio of the weighted mutation loads corresponding to population 0 and population 1. We calculate $\langle R \rangle$ for all non-synonymous sites, in addition to Polyphen classes, including benign, possibly damaging, and probably damaging sites (see tables below).

We calculated the expected $\langle R \rangle$ from simulations for four demographic models: Tennesen [3], Gravel [4], Lohmueller [5], and a simple bottleneck without exponential growth. We compare $\langle R \rangle$ from simulations with the R statistic observed in African Americans/European Americans from the Exome Sequencing Project (ESP) to assess the validity of different demographic models. Using this approach, we are unable to reject the Tennesen, Gravel and Lohmueller models, since $\langle R \rangle$ from these models are all within the 95% confidence intervals of R from ESP for all classes. The square bottleneck prediction is 2.09 standard errors from the empirical observation from the ESP measurement which is weakly suggestive that this model is not consistent with the data. These results suggest that this approach, the accumulation of deleterious mutations in two populations, along with the inferred DFE, can be a useful tool to evaluate the validity of different demographic models.

all non-synonymous sites	$\langle L \rangle_{pop0}$	$\langle L \rangle_{pop1}$	$\langle R \rangle$
Tennesen	0.000139	0.000140	0.989
Gravel	0.000138	0.000140	0.987
Lohmueller	0.000113	0.000114	0.992
Simple Bottleneck	0.000138	0.000141	0.978

benign	$\langle L \rangle_{pop0}$	$\langle L \rangle_{pop1}$	$\langle R \rangle$
Tennesen	0.000193	0.000195	0.990
Gravel	0.000192	0.000194	0.988
Lohmueller	0.000157	0.000158	0.993
Simple Bottleneck	0.000192	0.000196	0.979

possibly damaging	$\langle L \rangle_{pop0}$	$\langle L \rangle_{pop1}$	$\langle R \rangle$
Tennesen	0.000123	0.000125	0.985
Gravel	0.000123	0.000125	0.984
Lohmueller	0.000101	0.000103	0.989
Simple Bottleneck	0.000123	0.000126	0.973

probably damaging	$\langle L \rangle_{pop0}$	$\langle L \rangle_{pop1}$	$\langle R \rangle$
Tennessen	0.00006909	0.00006995	0.988
Gravel	0.00006887	0.00006982	0.986
Lohmueller	0.00005698	0.00005748	0.991
Simple Bottleneck	0.00006885	0.00007048	0.977

References

- [1] Gregory V. Kryukov, et al. Power of deep, all-exon resequencing for discovery of human trait genes. *Proc. Natl. Acad. Sci. U. S. A.*, 106 (10) 3871-3876, 2009.
- [2] S. Asthana, et al. Analysis of Sequence Conservation at Nucleotide Resolution. *PLoS Comput. Biol.*, 3(12): e254, 2007.
- [3] J. A. Tennessen, et al. Evolution and functional impact of rare coding variation from deep sequencing of human exomes. *Science*, 337(6090):64–69, 2012.
- [4] S. Gravel, et al. Demographic history and rare allele sharing among human populations. *Proc. Natl. Acad. Sci. U. S. A.*, 108:11983–11988, 2011.
- [5] K. E. Lohmueller, et al. Proportionally more deleterious genetic variation in European than in African populations. *Nature*, 451(7181):994–997, Feb. 2008.

Note S2

The proportion of non-synonymous sites is driven by neutral demographic history

We performed computer simulations of two models of demographic history (shown in Figure 2A) that differ qualitatively with regard to the history after the population split: (1) “Tennessen et al. 2012”¹, and (2) “Bottleneck and growth”. We tuned the parameters of the “Bottleneck and growth” model to match the Tennessen et al. model¹ both for the population split time (2,040 generations ago) and the final predicted heterozygosities at synonymous sites in both West Africans and Europeans.

There is an important qualitative difference between the two models. For Tennessen et al.¹, West African populations are larger than European populations for most of the history since their split, and thus selection against weakly deleterious mutations would be expected to operate less effectively in European history. For the Bottleneck and Growth model, the opposite is the case.

Table S2.1: Simulations of 19 selective coefficients

Weighting of selection coefficients under Boyko model				Tennessen et al. ¹ demographic model results				Bottleneck & growth demographic model results			
s	gamma density	bin width	Weight: proportional to (gamma) x (bin width)	segregating sites /bp	$L_{Afr-not-Eur}$	$L_{Eur-not-Afr}$	$R_{Afr/Eur}$	segregating sites /bp	$L_{Afr-not-Eur}$	$L_{Eur-not-Afr}$	$R_{Afr/Eur}$
-0.000001	1.8×10^{-1}	1.4×10^{-6}	0.029	2.8×10^{-3}	6.1×10^{-4}	6.1×10^{-4}	1	3.4×10^{-3}	6.2×10^{-4}	6.2×10^{-4}	1
-0.000002	1.1×10^{-1}	1.7×10^{-6}	0.021	2.8×10^{-3}	6.1×10^{-4}	6.1×10^{-4}	1	3.3×10^{-3}	6.1×10^{-4}	6.2×10^{-4}	1
-0.000005	5.1×10^{-2}	3.9×10^{-6}	0.022	2.8×10^{-3}	6.0×10^{-4}	6.0×10^{-4}	1	3.3×10^{-3}	6.1×10^{-4}	6.1×10^{-4}	1
-0.00001	2.9×10^{-2}	7.1×10^{-6}	0.023	2.7×10^{-3}	5.9×10^{-4}	5.9×10^{-4}	1	3.3×10^{-3}	5.9×10^{-4}	5.9×10^{-4}	1
-0.00002	1.7×10^{-2}	1.7×10^{-5}	0.033	2.6×10^{-3}	5.6×10^{-4}	5.6×10^{-4}	1	3.2×10^{-3}	5.6×10^{-4}	5.6×10^{-4}	0.99
-0.00005	8.2×10^{-3}	3.9×10^{-5}	0.036	2.3×10^{-3}	4.7×10^{-4}	4.8×10^{-4}	0.99	2.9×10^{-3}	4.7×10^{-4}	4.8×10^{-4}	0.99
-0.0001	4.7×10^{-3}	7.1×10^{-5}	0.037	1.9×10^{-3}	3.5×10^{-4}	3.6×10^{-4}	0.98	2.4×10^{-3}	3.5×10^{-4}	3.6×10^{-4}	0.97
-0.0002	2.7×10^{-3}	1.7×10^{-4}	0.053	1.4×10^{-3}	2.1×10^{-4}	2.1×10^{-4}	0.97	1.9×10^{-3}	2.1×10^{-4}	2.2×10^{-4}	0.95
-0.0005	1.3×10^{-3}	3.9×10^{-4}	0.057	8.7×10^{-4}	8.4×10^{-5}	8.9×10^{-5}	0.94	1.3×10^{-3}	8.3×10^{-5}	9.1×10^{-5}	0.91
-0.001	7.6×10^{-4}	7.1×10^{-4}	0.059	6.5×10^{-4}	4.1×10^{-5}	4.5×10^{-5}	0.92	9.8×10^{-4}	4.1×10^{-5}	4.6×10^{-5}	0.90
-0.002	4.3×10^{-4}	1.7×10^{-3}	0.084	4.9×10^{-4}	2.0×10^{-5}	2.2×10^{-5}	0.92	6.6×10^{-4}	2.0×10^{-5}	2.2×10^{-5}	0.94
-0.005	2.0×10^{-4}	3.9×10^{-3}	0.089	2.8×10^{-4}	8.0×10^{-6}	8.3×10^{-6}	0.97	3.0×10^{-4}	8.1×10^{-6}	8.1×10^{-6}	1
-0.01	1.1×10^{-4}	7.1×10^{-3}	0.090	1.6×10^{-4}	4.0×10^{-6}	4.0×10^{-6}	0.99	1.6×10^{-4}	4.0×10^{-6}	4.0×10^{-6}	1
-0.02	6.1×10^{-5}	1.7×10^{-2}	0.120	8.0×10^{-5}	2.0×10^{-6}	2.0×10^{-6}	1	7.9×10^{-5}	2.0×10^{-6}	2.0×10^{-6}	1
-0.05	2.4×10^{-5}	3.9×10^{-2}	0.105	3.2×10^{-5}	8.0×10^{-7}	8.0×10^{-7}	1	3.2×10^{-5}	8.0×10^{-7}	8.0×10^{-7}	1
-0.1	9.9×10^{-6}	7.1×10^{-2}	0.078	1.6×10^{-5}	4.0×10^{-7}	4.0×10^{-7}	1	1.6×10^{-5}	4.0×10^{-7}	4.0×10^{-7}	1
-0.2	2.9×10^{-6}	1.7×10^{-1}	0.056	8.0×10^{-6}	2.0×10^{-7}	2.0×10^{-7}	1	8.0×10^{-6}	2.0×10^{-7}	2.0×10^{-7}	1
-0.5	1.8×10^{-7}	3.9×10^{-1}	0.0077	3.2×10^{-6}	8.0×10^{-8}	8.0×10^{-8}	1	3.2×10^{-6}	8.0×10^{-8}	8.0×10^{-8}	1
-1	3.3×10^{-9}	2.9×10^{-1}	0.00011	1.6×10^{-6}	4.0×10^{-8}	4.0×10^{-8}	1	1.6×10^{-6}	4.0×10^{-8}	4.0×10^{-8}	1
Non-synonymous	N/A	1	1	7.6×10^{-4}	1.27×10^{-4}	1.29×10^{-4}	0.987	9.6×10^{-4}	1.28×10^{-4}	1.30×10^{-4}	0.983
Synonymous	N/A	N/A	N/A	2.8×10^{-3}	6.17×10^{-4}	6.17×10^{-4}	0.999	9.6×10^{-4}	6.21×10^{-4}	6.22×10^{-4}	0.998

We simulated 10 billion base pairs for a selection coefficient of $s = 0$ (“synonymous sites”) and 1 billion base pairs for each of 19 negative selection coefficients (“non-synonymous”) (Table S2.1). For the total number of segregating non-synonymous sites, we weighted each of the 19 selection coefficients based on an inferred distribution of human selection coefficients from

Boyko et al. 2008² (the fit to European genetic variation data, in which s follows a gamma distribution with $\alpha=0.206$ and $\beta=15400$). Specifically, we took the gamma density (“gamma density” in Table 1), and multiplied it by the range of selection coefficients represented by that bin (“bin width”). We renormalized these products so that they summed to one.

For each simulation, we tabulated the number of segregating sites per generation over the last 3000 generations of history assuming a sample size of 40 for both West Africans and 40 Europeans (we used a hypergeometric distribution to obtain the expected probability of each polymorphic site being heterozygous given that sample size).

To obtain numbers for all non-synonymous sites we used the weights shown in Table S2.1 to compute the expected rate of segregating sites per base pair in both West Africans and Europeans each generation.

To compute the proportion of non-synonymous sites in each generation, we used the following equation, with the factor of 3.42 chosen to be what was needed for the proportion equal to the empirical value in ref. ³ (0.479).

$$\text{proportion nonsynonymous} = \frac{3.42 \times \text{nonsynonymous}}{3.42 \times \text{nonsynonymous} + \text{synonymous}}$$

Figure 2B shows the temporal dynamics of the density of non-synonymous sites (per base pair), the density of synonymous sites, and the proportion of all sites that are non-synonymous. We only show results here for Europeans (in both simulated models, the West African population size changes very little and so the statistics hardly change, at least compared with Europeans).

Both simulated demographic models show the same qualitative feature as the simulations presented in ref. ³. Non-synonymous and synonymous segregating site densities are initially decreased in Europeans by the bottleneck for all classes of selection coefficients, with the proportional effect being larger for non-synonymous sites. In the recovery period, however, non-synonymous segregating site densities increase faster than synonymous ones. Thus, the total proportion of sites that are non-synonymous also increases in this period. In both simulated demographic models, the proportion of non-synonymous sites thus has a non-trivial behavior of initially falling and then rising, eventually passing the baseline.

Ref. ³ argued that the observation of an elevated rate of non-synonymous sites in present-day Europeans (compared with West Africans as a baseline) is evidence of less effective natural selection to remove weakly deleterious mutations in European than in West African populations since their separation. If this is the case, it is surprising that the Bottleneck and Growth model where population sizes have been larger in European than in West Africans populations for most of their history shows the same qualitative effect.

We modified the simulation so that in every generation, we simulated two values for the expected number of segregating sites in that generation.

$A_{s,i}$ = “All evolutionary forces”: Number of segregating sites in phenotypic class s (e.g. a particular selection coefficient, or all non-synonymous sites) in generation i
 $N_{s,i}$ = “No selection” Number of segregating sites in phenotypic class s in generation i , incorporating the effects of mutation and drift, but setting $s=0$ relative to generation $i-1$

We then define the proportion of sites that are non-synonymous in a given generation, which can be for a particular selection coefficient or integrating over a distribution of coefficients, as:

$$\begin{aligned} PropAll_i &= A_{s,i} / (A_{s,i} + A_{0,i}) \\ PropNeu_i &= N_{s,i} / (N_{s,i} + A_{0,i}) \end{aligned}$$

We computed expected values for three derivatives by summing up the following differences over all the simulation replicates.

$$\begin{aligned} \delta PropAll_i &= PropAll_i - PropAll_{i-1} \\ &\text{“All evolutionary forces”}: \text{change in the proportion of non-synonymous sites in} \\ &\text{generation } i \text{ compared to } i-1, \text{ incorporating the effects of mutation, drift and selection.} \\ \delta PropNeu_i &= PropNeu_i - PropAll_{i-1} \\ &\text{“neutral forces”}: \text{change in the proportion of non-synonymous sites in generation } i \\ &\text{compared to } i-1, \text{ incorporating the effects of drift and mutation only} \\ \delta PropSel_i &= PropAll_i - PropNeu_{i-1} \\ &\text{“selection forces”}: \text{change in the proportion of non-synonymous sites in generation } i \\ &\text{compared to } i-1, \text{ isolating the effects of selection.} \end{aligned}$$

Note that $\delta PropAll_i = \delta PropNeu_i + \delta PropSel_i$. Thus, we can partition the change in these quantities over time in terms of the effects of drift and mutation ($\delta PropNeu_i$), and the effects of selection ($\delta PropSel_i$).

In the ancestral population, $\delta PropAll_i = 0$, that is, the total proportion of sites that are non-synonymous is unchanging since the population is at mutation-drift-selection equilibrium. However, our partitioning allows us to quantify the fact that this equilibrium is in fact a balance of two pressures: the pressure to increase $PropNeu_i$ in any generation due to neutral forces (new mutations which are not all lost through drift) is exactly compensated by selection decreasing it. We empirically measure in our simulations that these per-generation pressures are:

$$\delta PropNeu_{baseline} = -\delta PropSel_{baseline} = 0.0000939 \text{ / base pair / generation}$$

What interests us in any generation is not these baseline rates of change attributable to neutral or selective forces, but instead how the change in the effectiveness of different evolutionary forces compares to the baseline. Thus, we define new quantities for the change per generation compared to baseline, allowing us to study how changes in $PropAll_i$ over time partition into effects due to weakening or strengthening of neutral or selective forces.

$$\begin{aligned} \Delta PropAll_i &= \delta PropAll_i && \text{“All evolutionary forces”} \\ \Delta PropNeu_i &= \delta PropNeu_i - \delta PropNeu_{baseline} && \text{“Neutral forces”} \\ \Delta PropSel_i &= \delta PropSel_i - \delta PropSel_{baseline} && \text{“Selective forces”} \end{aligned}$$

Figure 2C shows that the change in $\Delta PropAll_i$ (the expected change per generation due to all evolutionary forces) is highly correlated to $\Delta PropNeu_i$ (the expected change due to neutral forces) over all time periods. The effect of selection $\Delta PropSel$ is anti-correlated (Table S2.2).

Table S2.2: Correlation coefficients show that neutral forces drive the observed change in the proportion of non-synonymous sites per generation

Correlation ρ of $\Delta PropAll_i$ to	Tennessen et al. ¹ model	Bottleneck and growth model
<i>Neutral forces: $\Delta PropNeu_i$</i>	0.98	0.96
<i>Selection forces: $\Delta PropNeu_i$</i>	-0.40	-0.76

Another way to see this is through the bottom row of the simulation (Figure 2D), which shows the cumulative effect of each evolutionary force by integrating over all the generations since the population split. We observe that while the temporal dynamics are quite different in the two scenarios, in both scenarios, the proportion of non-synonymous sites in the present generation is higher for Europeans than for Africans.

We conclude with an intuition. Why are neutral forces the main driver of a rise in the proportion of sites that are non-synonymous after the European bottleneck?

The key intuition is that prior to the West African / European population split, the density of non-synonymous segregating sites is expected to have been much lower than the density of synonymous segregating sites due to the action of natural selection. This pattern would only have been intensified by the preferential loss of segregating sites for the non-synonymous class due to the out-of-Africa bottleneck as our simulations show (Figure 2B).

Once the population began expanding, drift would have been reduced and equilibrium would have favored a higher density of segregating sites both for non-synonymous and synonymous classes. The non-synonymous site class approaches its equilibrium relatively more quickly than the synonymous site class once population grows, as the non-synonymous class experiences the same flux of new mutations as synonymous sites. Since non-synonymous sites start out with a lower baseline density, the proportional rate of their approach to equilibrium is faster than for synonymous segregating sites, explaining our observation. Selected classes of mutations turn over more quickly, and thus approach equilibrium more quickly⁴.

References for Note S2

1. Tennessen, J.A. *et al.* Evolution and functional impact of rare coding variation from deep sequencing of human exomes. *Science* **337**, 64-9 (2012).
2. Boyko, A.R. *et al.* Assessing the evolutionary impact of amino acid mutations in the human genome. *PLoS Genet* **4**, e1000083 (2008).
3. Lohmueller, K.E. *et al.* Proportionally more deleterious genetic variation in European than in African populations. *Nature* **451**, 994-7 (2008).
4. Reich, D.E. & Lander, E.S. On the allelic spectrum of human disease. *Trends Genet* **17**, 502-10 (2001).